McMaster University

School of Graduate Studies
Final Thesis Submission Sheet
Updated June 2024

First Name: Zahan **Last Name:** Cooper

Student ID Number: 400017107 **Program:** Chem Eng **Degree:** MASc

Supervisor: Heather Sheardown **Defence Date:** 2024-12-19

Convocation Ceremony Deadline Dates

Congratulations on this major milestone! The Sessional Dates in the Graduate Calendar specify the "Final Date to File Theses with Graduate Studies and Complete Degree Requirements" which is when you must upload your final thesis to MacSphere to join the ceremony, Fall or Spring. If you upload your thesis past the noted deadline, for example September 29 for Fall 2023, but prior to the ceremony date (e.g. Fall November Convocation), you are required to email the Associate Registrar at areggrad@mcmaster.ca to request that you join convocation and indicate that you have completed your degree requirements. Should you be approved to join late, your ceremony experience may be impacted.

In addition to the email, you can use the following check box to clearly identify your convocation ceremony preference if you fall into the above mentioned time frame from deadline to ceremony.

Convocation Ceremony Preference: ☐ Fall Convocation ☑ Spring Convocation

Please note: this is **NOT** a deferral of ceremony request. The expectation is that you join the ceremony in which your degree requirements were cleared for. If you were unable to attend your designated ceremony, you must submit a Service Request for the deferral of your ceremony and you should recognize that your degree would have already been conferred at the past ceremony.

Once you have uploaded your FINAL thesis on MacSphere and your completed form has been submitted to the Graduate Administrator for your program, you can be cleared to graduate, provided all other program requirements are complete. From that date on, you are no longer considered an active Graduate student and the tuition balance of the months remaining in the academic year will be refunded.
Please note: Once your thesis is approved and posted to MacSphere, no changes are permitted.

Does this thesis require a delay of publication? ☐ Yes ☑ No

You may request up to one year. Failure to complete this box will result in your thesis being posted publicly immediately. Please indicate the length of embargo if less than one year:

Supervisor's Signature	**Student's Signature**

Plagiarism Check

Students who initiate their defence on or after December 1, 2023 are required to run their thesis through the University's Plagiarism Checking Software, iThenticate.

I confirm that this thesis has been checked using the University's designated Plagiarism Checking Software.

Supervisor's Signature	**Student's Signature**

This sheet must accompany the final submission of the thesis to the School of Graduate Studies following a successful defence

To the Defence Chair: Please indicate by initialing the appropriate box which of the conditions pertain to the successful defended PhD thesis. Then please give this form to the student to complete and submit along with the revised thesis to the School of Graduate Studies.

○ No Changes Required

The thesis needs no further changes.

Supervisor's Name

Date	**Signature**

◉ Minor Changes Required

The thesis requires minor changes (typographical errors, minor corrections). The Supervisor has agreed to act on behalf of the Defence Committee and ensure that the required changes have been made. I have seen the revised thesis and acknowledge that all necessary and request changes have been made.

Please list the minor changes below:
Additional graph
Minor additions to the introduction and conclusions

Supervisor's Name Heather Sheardown

Date 2024-12-24	**Signature** 

○ Major Changes Required

The thesis requires major changes more than just in style. The entire Supervisory Committee must approve the revised thesis.

Please list the major changes below:

By signing below, we the Supervisory Committee, have seen the revised thesis and acknowledge that all the necessary and requested changes have been made.			
	Printed Name	**Signature**	**Date**
Supervisor's Name	Heather Sheardown		
Committee Member Name	Ryan Wylie		
Committee Member Name	Stuart Linley		
Committee Member Name			

Once this form is fully complete, please submit via Service Request
Final Thesis Submission Sheet - FTHS

McMaster University

License to McMaster University

Updated June 2022

First Name: Zahan

Family Name: Cooper

Program: Chemical Engineering

Degree: Masters in Applied Science (MASc)

Supervisor: Dr. Heather Sheardown

Defence date: 12/19/2024

In the interests of facilitating research by others at this institution and elsewhere, and in consideration of my being accepted for enrolment as a graduate student at this institution, I hereby grant a license to:

McMaster University

to make copies of my graduate thesis/dissertation (for substantial parts thereof) and to reproduce it on the web (or any future method of dissemination), the copyright of which is vested in me, provided that this licence is subject to the following conditions:

1. Only single copies shall be made or authorized to be made at any one time, and only in response to a request from the library or any university or similar institution on its own behalf or on behalf of one of its users.

2. This licence shall continue for the full term of the copyright, or for as long as may be legally permitted.

3. The Universal Copyright Notice shall appear on all copies made under the authority of this licence.

4. This licence does not permit the sale of authorized copies at a profit, but does permit the collection by the institution or institutions concerned of charges covering actual cost.

5. All copies made under the authority of the licence bear a statement to the effect that the copy in question "is being made available in this form by authority of the copyright owner solely for the purposes of private study and research and may not be copied or reproduced except as permitted by the copyright laws without written authority from the copyright owner".

6. The foregoing shall in no way preclude the granting by the author of a licence to the National Library of Canada to reproduce the thesis or dissertation and to lend or to sell copies of the same. For this purpose it shall also be permissible for McMaster University to submit the above mentioned thesis or dissertation to the National Library of Canada.

Signature of Witness

Signature of Student

Date

Date 12/24/2024

3D-Printed Therapeutic Vitamin E Bandage Contact Lenses

3D-Printed Therapeutic Vitamin E Bandage Contact Lenses

Author: Zahan Cooper (McMaster University)

Supervisor: Dr. Heather Sheardown

McMaster University

Department of Chemical Engineering

Hamilton, ON, Canada

A Thesis Submitted to the School of Graduate Studies In the Partial Fulfillment of the Requirements For the Degree Master of Applied Science

MASTER OF APPLIED SCIENCE (2024) McMaster University

Department of Chemical Engineering Hamilton, Ontario, Canada

TITLE: 3D-Printed Therapeutic Vitamin E Bandage Contact Lenses

AUTHOR: Zahan Kayomerd Cooper, BASc (McMaster University)

SUPERVISOR: Dr. Heather Sheardown

NUMBER OF PAGES: xii, 76

Abstract

The ocular surface is extremely effective at protecting the eye through such physiological barriers as the cornea and tear film. The exposed nature of the cornea can still lead to a significant number of injuries and harm from the external environment. Management and treatment of ocular injuries involves a combination of a bandage contact lens (BCL) along with therapeutic eye drops that require frequent and strict dosing regimens that can be difficult to maintain and are inefficient due to the high clearance rate of the eye. Therapeutic contact lenses (TCL) with vitamin E (VE) incorporated have been shown to steadily release a desired therapeutic agent and potentially simplify a patient's treatment process. Vat polymerization (VP), a form of 3D printing, was utilized in this work to explore a platform design for developing customizable VE-containing TCLs, using dexamethasone phosphate (DXP) as a model drug. VP was also used to explore the creation of a multi-material TCL, using a VE embedded ring that could be directly printed within the lens in a streamlined and automated manner.

Three lens formulations consisting primarily of hydroxy ethyl methacrylate (HEMA) and polyethylene glycol diacrylate (PEGDA) with modified formulations containing methacrylated VE (VEMA) and Methacryloxypropyltris (Trimethylsiloxy) silane (TRIS) as a model silicone material were prepared. These lenses were synthesized and characterized to examine 3D printing for lens creation in comparison to commercial standards. The base and VEMA formulations were used to examine the feasibility of a multi-material (MM) lens with an embedded ring directly incorporated during the printing process.

All three formulations showed shear thinning properties suitable for VP bioprinting applications. The base formulation produced a very homogenous print while VEMA prints showed defects and clear phase separation. The VEMA+TRIS formulation showed significant

improvement as the prints were more homogenous with fewer defects. The MM lenses showed a mixture of properties between the base and VEMA formulations, with the center appearing more homogenous and the edge that included the embedded ring showing defects similar to VEMA prints.

Surface wettability and water content decreased from the base formulation with an increasing presence of hydrophobic moieties in the modified formulations. The increased hydrophobicity can be correlated with an increase in stiffness seen from the base formulation. While all materials had high moduli due to the high crosslinking density and presence of PEGDA, the VEMA prints had a higher modulus than the base material but were quite brittle due to the increased hydrophobicity and poor print quality. The VEMA+TRIS prints showed a significant ($p < 0.05$) increase in stiffness without the brittleness of the VEMA prints due to the better print quality. The MM prints had the lowest moduli, most similar to the base material, indicating that this lens design could mitigate the brittleness seen with the VEMA prints. A comparison of 3DP and casting showed the cast material having a significantly ($p < 0.05$) higher modulus than the 3DP material presumably due to the bulk vs. layer-by-layer polymerization processes that the respective manufacturing methods utilize. The base material produced significantly more transparent prints, with transmissions (wavelength) that ranged between 80-88%, compared to the VEMA and VEMA+TRIS prints which ranged from 18-47%. The MM lenses showed promise for minimizing the effect of the poor transparency of the VEMA ring with transparency of 62-85%. Besides the formulations, the lens thickness, print quality and print plate surface were found to be major contributors to the printed lenses not meeting commercial standards.

The VEMA+TRIS loaded lenses showed the greatest changes in the release kinetics with a larger burst release, attributed to the weaker affinity DXP has to the hydrophobic components,

while the base and VEMA lens' profiles were very similar. The weaker drug-polymer interaction and more mobile silicone-oxygen bonds of TRIS are likely the reason for the VEMA+TRIS formulation releasing significantly more DXP than the base or VEMA lenses, with 69.21 ± 3.62%, 44.09 ± 4.63% and 37.09 ± 4.81% released respectively. It is believed that the high degree of crosslinking within the lens polymer matrix causes high levels of physical entrapment, resulting in an incomplete release of DXP from the lenses. Another possibility is that some DXP reacted with the acrylate components of the lens formulations as the photopolymerization process creates free radicals which could lead to the formation of covalent bonds of DXP with one of the monomers in the formulation.

The use of 3DP to develop customizable TCLs on-demand has a lot of potential as the biomedical and healthcare industries shift to more of a personalized rather than a one-size-fits all approach. The MM lens design allows for the incorporation of materials with poor lens properties without significantly impacting the lens' functions such as its tensile stiffness and transparency. The freedom of design that 3DP provides will allow for tailor-made lenses that can meet a patient's specific needs, including lens fitting, which would maximize the patient's comfort.

Acknowledgements

I'd like to thank my supervisor, Dr. Heather Sheardown for showing an ever-lasting sense of patience with me throughout this project as I worked to find my feet at McMaster. Thank you for giving me a unique opportunity with exploring this very novel area that was new to both me and this field while providing me the free reign to create my own project out of it. Thank you for sending me to ARVO which really allowed me to appreciate my work and gain confidence in my abilities.

Thank you to all of the members of the Sheardown Lab who have taught me the various lab techniques that have gotten me through it all. A big shout out to Lina, the fairy godmother of the lab, who has always provided a helping hand and insightful advice that has guided me through my Masters. Thank you to Mitch and Nate who helped me get settled into the grad school life at McMaster and being awesome roommates, even if it was only for a short time. Thank you to my friends and family who have supported and encouraged me throughout the process.

Table of Contents

List of Figures

List of Tables

List of Abbreviations

CL	Contact Lens
TCL	Therapeutic Contact Lens
BCL	Bandage Contact Lens
VE	Vitamin E/ δ-Tocopherol
3DP	3D Printing
VEMA	Methacrylated/Printable Vitamin E
VP	Vat Polymerization
HEMA	Hydroxy ethyl methacrylate
PEGDA	Polyethylene glycol diacrylate
TRIS	Methacryloxypropyltris (Trimethylsiloxy) silane
DXP	Dexamethasone phosphate
MM	Multi-material
PEG	Polyethylene glycol
DDS	Drug delivery systems
PMMA	Polymethylmethacrylate
EGDMA	Ethylene glycol dimethacrylate
SiHys	Silicone-based Hydrogels
UV	Ultraviolet
DDS	Drug delivery system
TPGS	D-alpha-tocopheryl polyethylene glycol 1000 succinate
(M)SLA	(Masked) Sterelothiography
DLP	Digital Light Processing
LAP	Lithium phenyl-2,4,6-trimethylbenzoylphosphinate
FDM	Fusion Deposition Modelling
NMR	Nuclear Magnetic Resonance
TEM	Transmission Electron Microscopy

1. Introduction

1.1 Ocular Conditions and Current Treatment Approach

Ocular diseases, like cataracts and glaucoma, and subsequent vision impairment have been on the rise over the past decade, impacting an estimated 2.2 billion people globally and 5.5 million Canadians [1, 2]. Ocular injuries, primarily corneal abrasions and chemical burns, account for 3% of all emergency visits as the eye is exposed to the external environment and is vulnerable to these types of injuries. Treatment of ocular diseases and injuries typically requires patients to follow very strict eye drop regimens. These regimens are also necessary either before or after a surgical procedure. Eye drops provide pulsatile delivery of an instilled drug, with less than 5% of the drop reaching the cornea and a high dose self-administered that remains in the therapeutic window for a very short time, resulting in the need for frequent doses as seen in Figure 1 [3]. The need for frequent administration, combined with the difficulty of self-administration lead to low patient compliance that can contribute to further complications after a traumatic injury or surgery [3]. Despite this, topical solutions account for over 90% of all ophthalmic medications [3]. Therefore, a more efficient means of ocular drug delivery that would improve patient compliance and patient outcomes leading to a dramatic effect on the growing rate of visual impairment, globally [1].

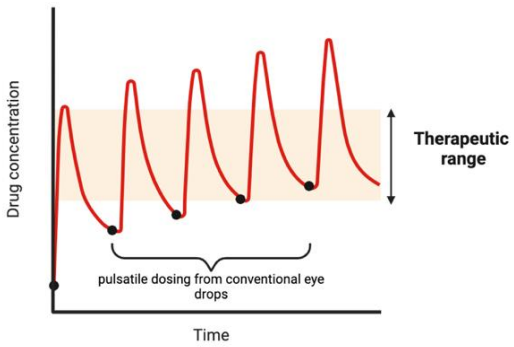

Figure 1: Drug concentration profile for conventional ophthalmic topical solutions created with biorender.com

1.2 Therapeutic Contact Lenses

Therapeutic contact lenses (TCLs) have significant promise to improve therapeutic outcomes, with the additional potential to act as reservoirs for drugs, significantly improving the residence time of a drug on the ocular surface [4]. It has been suggested that as much as 95% of an instilled eye drop is cleared from the eye through blinking and other clearance mechanisms within five minutes of administration [4]. Contact lenses have been used to aid corneal wound healing and recovery following ocular trauma or surgery since the 1970s, when Bandage CLs (BCLs) were first introduced, [5, 6]. They provide a physical barrier that can minimize potential infection and further irritation or damage caused by the external environment, allowing for corneal wound healing. As the BCLs have to be worn for extended periods, strict antibiotic and corticosteroid eye drops regimens are prescribed to prevent infection and inflammation while the wound is healing, which patients may struggle to maintain [5, 6]. TCLs can potentially mitigate this as they can potentially act as reservoirs for multiple therapeutic agents that are released over an extended period to absolve the frequent, pulsatile overdosing regimen that users experience with eye drops.

1.3 Vitamin E

Vitamin E (VE) is a group of lipid-soluble compounds that are naturally found in vegetables, nuts and oils [7]. They have shown to prevent and manage various ocular disorders like glaucoma and cataracts due to antioxidant and anti-inflammatory effects [7]. Vitamin E has been used in contact lenses to control drug delivery through the creation of barriers [8]. Others have included Vitamin E into TCLs to create a hydrophobic diffusion barrier that reduces the rate of release of therapeutic agents, particularly hydrophilic drugs [9]. Despite the promise it shows

for controlling drug delivery, VE incorporation into lenses has been shown to impact material and mechanical properties, decreasing transparency and oxygen permeability at higher concentrations [9]. However, current methods of mass production lack the ability to incorporate design flexibility that may help alleviate these issues [10].

1.4 3D Printing in Biomedical Applications

3D printing (3DP) offers a high degree of customizability for both design and material incorporation as it offers significant control of the manufacturing process leading to rapid growth of its use in the biomedical field over the past two decades [10-12]. It has already been utilized in creating patient-specific devices, particularly wearable medical devices or prostheses [11, 12]. The growing trend of personalized medicine has seen its use be examined in more advanced areas, namely pharmaceutical manufacturing and tissue engineering [11, 12]. 3DP provides a means to generate tailor-made therapies based on patient needs which mass manufacturing systems cannot achieve [11, 13].

While extrusion-based 3DP has been the most widely used method, vat polymerization (VP) has shown great promise with high printing resolution at rapid speeds, enabling fast batches of tailor-made therapeutic devices to be produced [14, 15]. It also offers control of the material make-up of an object for each layer as the printer cures objects in a layer by layer manner [10]. These principles have seen VP be used in created microfluidic devices for rapid drug screening and disease modelling, creating accurate organ models for regenerative medicine, and pharmaceuticals with complex designs that is capable of incorporating multiple therapeutic agents [11, 14]. VP has begun to be examined in ophthalmology, mainly for creating corneal or retinal models and prostheses, with its use in contact lens manufacturing starting to be explored [15-17].

1.5 Thesis Rationale

The aim of this thesis is therefore to explore a platform design for developing 3DP TCLs and creating a multi-material (MM) contact lens that maintains important mechanical and physical aspects like the tensile properties and lens transparency. Three lens formulations were devised, mainly consisted of hydroxy ethyl methacrylate (HEMA) and polyethylene glycol diacrylate (PEGDA) with modified formulations containing a printable VE (VEMA) and another with VEMA and methacryloxypropyltris (Trimethylsiloxy) silane (TRIS) as a model silicone material. This method allows for direct VE incorporation in the lens matrix rather requiring incorporation through lens soaking which allows for direct control of VE loading. Furthermore, the layer-by-layer printing process was utilized to create a multi-material lens with an embedded ring made of the VE modified formulation to allow for and control drug release. Modified materials were compared against the single material lenses for mechanical and physical properties. The single material lenses were further evaluated for their potential as TCLs by examining their drug release profiles using dexamethasone phosphate (DXP) as a model drug. This work explores the use of 3DP as a new manufacturing alternative to current methods for CLs, develop and examine printable CL formulations. While 3DP cannot meet the output volume of mass manufacturing methods, it offers customizability with precise dimensional control that allows for custom-fit lenses with ease and minimal post-processing. The single and MM lens further displays the potential of developing personalized, on-demand TCLs capable of incorporating and localizing the dispersion multiple therapeutics. Drug release profiles can be tuned with direct control over drug loading and material selection and lens design to tailor it to a patient's specific needs.

2. Literature Review

2.1 Overview of the Function of the Eye

The function of the eye is the translation of light into electrical signals which can be transmitted to the brain. This involves a myriad of interactions between various cell types. The eye itself can be split into the anterior and posterior segments, with the former consisting of the sclera, conjunctiva, cornea, aqueous chamber, iris, pupil and lens as seen in Figure 2 [18]. The latter is made up of the choroid, retina, optic nerve, vitreous humour and the posterior chamber. The anterior segment provides protection for the internal structures of the eye from external factors in addition to enabling the passage and focusing of light [18]. More than 70% of the focusing power of the eye comes from the cornea, with the rest coming from the lens [19]. Once the light is focused onto the retina, it is converted to an electrical signal which is transmitted to the brain via the optic nerve.

2.2 Anterior Ocular Surface

The Anterior Ocular surface consists of four major components: the sclera, conjunctiva, cornea and tear film, all with the primary function of providing a protective barrier for the eye from the external environment, as shown in Figure 2 [19, 20]. The conjunctiva is a translucent mucous membrane overlying the stroma that provides a physical barrier to pathogens and foreign bodies, mechanical strength and produces tear constituents [19, 20]. It connects to the sclera, a white opaque tissue covering the eye in both the posterior and anterior regions that protects the intraocular contents from traumatic injury and mechanical displacement [21].

2.2.1 Cornea

The cornea is an avascular connective tissue that contributes two-thirds of the refractive power of the eye. Along with the sclera, it acts as the structural barrier and protects the eye against infections [19, 22]. The cornea is comprised of three cellular layers: epithelium, stroma and endothelium along with two interfacing layers, Bowman's membrane and Descemet's membrane, shown in Figure 2 [19, 22].

2.2.1.1 Epithelium

The corneal epithelium is a 50µm thick, transparent superficial layer of the cornea. It acts as a physical barrier to protect the stroma and internal ocular structures from the external environment [22, 23]. The epithelium made up of three cell types: superficial, wing and basal cells. Cell turnover in the epithelial layer is typically a 7-10 day process, with deeper cells replacing the desquamated superficial cells in a continuous cycle [23]. Superficial cells are 2-3 layers of flat cells with microvilli and microplicae coated by a charged glycocalyx layer that increases surface area and facilitates interaction between the cornea and mucin layer of the tear film [19, 22]. Adjacent superficial cells have tight junctions between, and as a. result they act as a permeability barrier to limit and regulate the entry of tears, chemicals and microbes into the deeper layers of the cornea. Wing cells make up the 2-3 layers under superficial cells and have the same functionality but are less flat and lack any projections. Basal cells are the deepest layer consisting of a single layer of columnar epithelial cells, approximately 20µm thick [19, 22]. They are the source of both wing and superficial cells and are the only corneal epithelial cells capable of mitosis [23]. Bowman's membrane is slightly adherent to the basement membrane and lies between the corneal epithelium and stroma [22]. This acellular layer is made of collagen types I and V as well as proteoglycans to create a smooth layer that maintains the shape of the cornea and aids with corneal

transparency. While it has strong resistance to injury, it has no regenerative ability and wounding generally leads to scarring [23]. While the primary function of Bowman's membrane is unknown, it has been suggested that it acts as a physical barrier to the subepithelial nerve plexus, protecting the stroma from direct trauma and the spread of microbial infections [23].

2.2.1.2 Stroma

The corneal stroma is approximately 500 µm thick, making up the bulk of the structural framework, contributing 80-85% of the cornea's thickness and playing an essential role in structural integrity [19, 22]. This transparent layer is comprised of primarily Type 1 collagen fibrils arranged in a precise manner, along with other extracellular matrix proteins. This network of stacked lamellae arranged parallel to one another reduces light scattering while contributing to the mechanical strength and structural integrity of the cornea [19, 22]. Anterior stromal rigidity is vital for maintaining corneal curvature and with a tighter arrangement of collagen fibers in this region over the posterior which is more prone to developing folds [23]. The main cell type of the stroma, keratocytes, contribute about 10% of the stroma's volume and are responsible for maintaining the extracellular matrix and collagen fibrils. The anterior stromal region is more populated with keratocytes than the posterior, further highlighting the importance of the anterior stromal region [19, 22].

2.2.1.3 Endothelium

The endothelium consists of a cellular monolayer of hexagonal, metabolically active cells, located at the posterior surface of the cornea [19, 22]. It is attached to the rest of the cornea through Descemet's membrane, a continuous, uniform layer of elastic collagenous fibers that is maintained by these endothelial cells. Corneal clarity is maintained by these endothelial cells through their role in keeping the stroma in a deturgesced state [19, 22]. This is dehydration mediated by the

"pump-leak" process whereby the endothelium maintains the levels of fluid, solutes and nutrients in the anterior region of the cornea [19, 22].

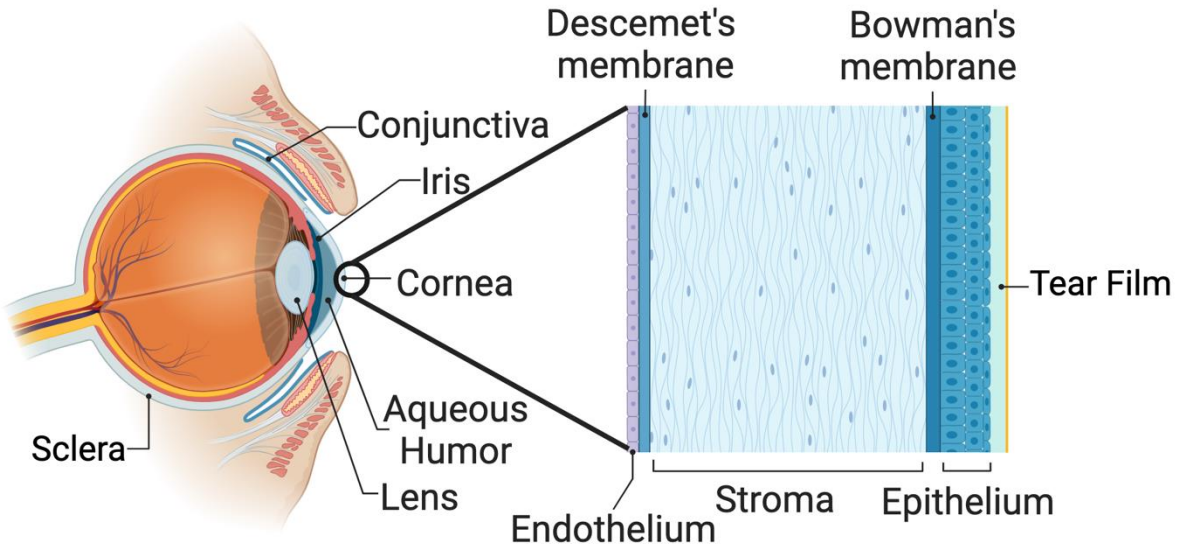

Figure 2: Anatomy of the ocular surface and cornea created with biorender.com

2.2.2 Tear Film

The tear film is roughly 3µm thick and has a volume of 3-10µL. It is responsible for lubrication of the ocular surface, aiding the cornea with light refraction as well as maintaining corneal and conjunctival homeostasis [24]. Figure 3 shows the trilaminar structure consisting of an outer lipid layer, an intermediate aqueous layer and an inner mucin layer.

The mucin layer is produced by secreted and transmembrane mucins originating from the conjunctival and corneal epithelial cells, the lacrimal gland and goblet cells within the conjunctival epithelium [24, 25]. These transmembrane mucins anchor the aqueous layer of the tears to the corneal epithelium with the aid of the corneal glycocalyx to allow for uniform lubrication of the ocular surface. The glycocalyx also acts as a physical barrier to pathogens [24, 25]. Soluble mucins

are also found in the aqueous layer, with a steadily decreasing concentration, decreasing surface tension and viscosity of the overlying tear film to improve its wettability [24, 25].

The aqueous layer of the tear film is produced by the lacrimal glands and is composed predominately of water along with electrolytes, vitamins, proteins, peptides and growth factors like epidermal growth factors [24, 25]. This layer is essential for hydration, lubrication and protection the ocular surface from foreign bodies while also providing nourishment for the cornea. The mucin and aqueous layers both house antimicrobial proteins, enzymes and immunoglobulins that aid the immune system of the ocular surface.

The lipid layer is a thin layer that interacts most with the external environment and plays a vital role in controlling the rate of tear evaporation and protection from dust particles [24, 25]. It consists of cholesterol, fatty acids and phospholipids, primarily produced by meibomian glands within the eyelids. This layer further reduces the surface tension of the aqueous phase to minimize disruptions caused by movement of the eye or eyelids to maintain a constantly smooth ocular surface.

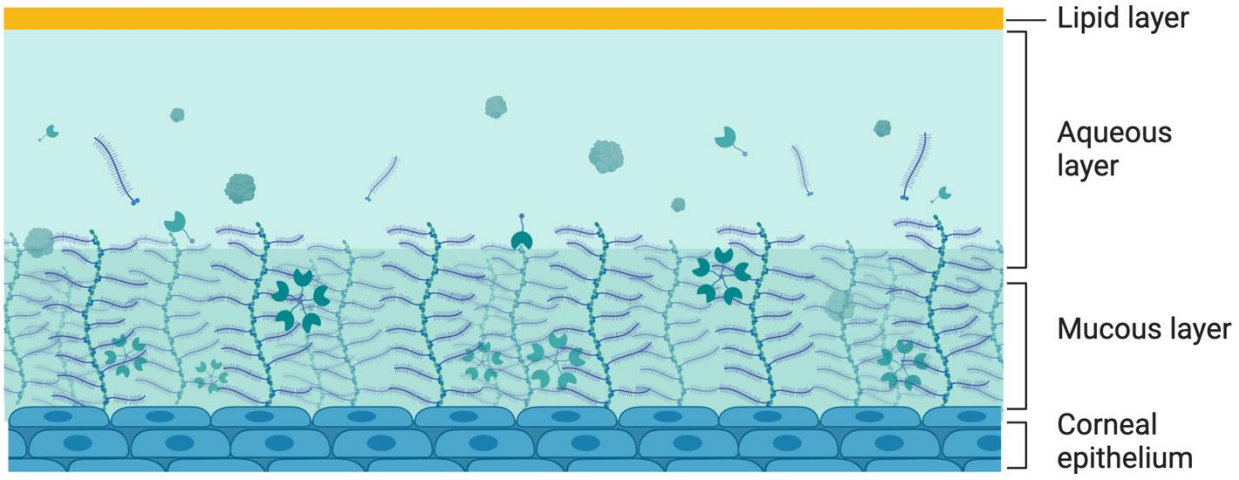

Figure 3: Tear film structures created with biorender.com

2.3 Drug Delivery Challenges in the Anterior Segment

There are a wide breadth of ocular drug delivery methods currently utilized to administer therapeutic agents to the eye, with topical administration being by far the most common. Topically administered drugs account for roughly 90% of all commercially available ophthalmic therapeutics yet they have a very low therapeutic effect, with less than 5% of any instilled drug being retained just five minutes after administration [26].

Several precorneal factors limit the effectiveness of topically applied drugs. Blinking along with the high tear turnover rate and drainage into the nasolacrimal system contribute to the high clearance rate of topically applied drugs [26]. The varying polarity of the lipid and aqueous layer of the tear film further limit the penetration of therapeutic agents through the various layers, particularly hydrophilic drugs due to the external lipophilic layer [24, 26]. Furthermore, the mucin layer limits permeation of drugs to the ocular surface as drugs bound to the mucin layer are cleared with each blink. The tight junctions of the cornea act as a physical barrier that limit diffusion through the various layers of the cornea [22, 26]. The cornea itself has five layers of varying polarity and permeability, making it difficult for both hydrophilic and hydrophobic drugs to penetrate [26].

A few different alternatives have been explored to overcome these barriers, including permeation enhancers, mucoadhesive polymers, nanoparticles and even microneedles [4, 26]. Permeation enhancers work by either improving drug solubility or by disrupting the protective membranes of the tear film and cornea [4, 26]. Polyethylene glycol (PEG) is an example of a permeation enhancer that improves the solubility of a drug while surfactants like palmitoyl carnitine improve permeation through cellular membranes and transcellular pathways [26]. Mucoadhesive polymers increase the residence time of a therapeutic agent within the tear film as

the polymer binds to the mucosal layer and prevents the rapid clearance of the therapeutic agent [4, 26]. Nanoparticles can adopt both properties and can also increase the penetration of the therapeutic agent through the physical barriers. While these microscopic systems can improve drug delivery, the clearance mechanisms still significantly limit their effectiveness [4, 26].

To minimize these losses and to increase the residence time the therapeutic agent has with the cornea, macroscopic systems have been explored as drug reservoirs, either in combination with the microscopic systems or as a stand-alone drug delivery systems (DDS) [4, 26]. An example of this is intracorneal microneedles which can bypass the physiological and physical barriers of the ocular surface [26]. For example, a study utilizing fluorescein-coated microneedles showed a much higher concentration of the fluorescein being delivered to the cornea than via topical application [26]. Contact lenses have long been suggested as potential drug reservoirs with studies going back as early as 1965 [4, 26]. Extensive work has been performed utilizing various materials or in combination with microscopic systems to enhance ocular drug delivery.

2.4 Contact Lenses

The first wearable contact lenses (CLs) began as glass-blown shells as early as 1888 but these were found to be heavy and limit tear exchange [27]. Glass scleral lenses were the status quo until the development of polymer-based CLs, generally made with polymethylmethacrylate (PMMA) in the 1940s, known as hard or rigid CLs [28, 29]. PMMA CLs were troublesome due to their poor oxygen permeability, but modern-day rigid gas permeable (RGP) CLs have moved away from PMMA. While early RGPs had good oxygen permeability, patients often experienced discomfort due to the lens stiffness. Later iterations of RGPs became softer with the addition of low-modulus components but patients still experienced discomfort due to the poor wettability of the lenses [28]. Following the discovery of hydroxy ethyl methacrylate (HEMA) in the 1960s,

there was a rapid rise in the popularity of soft contact lenses as their high water content allowed for greater material flexibility and sufficient oxygen permeability, thus providing more comfort to their RGP counterpart [28]. This hydrophilic and biologically inert monomer was responsible for this shift and has become a core material in a multitude of commercially available soft contact lenses today [28, 29].

2.4.1 Soft CL Materials

HEMA-based CLs are known for their high-water content, ranging between 20-80% based on the comonomers used in the lens formulation [28]. Ethylene glycol dimethacrylate (EGDMA) is commonly incorporated to improve mechanical properties of a lens by increasing the degree of cross-linking. However, there is generally an inverse correlation between crosslinking density and water content or oxygen permeability, as the increased crosslinking results in a more rigid hydrogel network. Methacrylic acid (MAA) and N-vinyl pyrrolidone (NVP) are hydrophilic comonomers added to increase the water content due to their functional groups [28]. Polyvinyl alcohol (PVA) has shown a higher degree of wettability than MAA or NVP. HEMA CLs are very modifiable, allowing for a variety of formulations that are optimized to achieve desirable CL attributes, but the relatively low oxygen permeability limits them to daily wear.

Silicone-based hydrogels (SiHys) emerged as the new frontrunners of the contact lens field due to their high oxygen permeability, enabling long wear times without risking hypoxia [28, 29]. Methacryloxypropyltris (Trimethylsiloxy) silane (TRIS) is short-chain acrylated siloxane that is commonly used in silicone-based hydrogel lenses. The silicone-oxygen (Si-O) bonds are more flexible than carbon-carbon bonds, allowing for greater gas permeability through the membrane of the hydrogel [28-30]. These more mobile bonds lower the wettability of CLs as the Si-O bonds move to the surface of the hydrogel, often leading to dryness and discomfort for users. Various

methods, including post-processing with plasma surface treatment or incorporating wetting agents have been used to improve the wettability of SiHy's [28-30]. Poly (ethylene glycol) (PEG) derivatives have been used in HEMA and SiHy CLs to alter properties such as wettability and mechanical strength while offering anti-fouling characteristics to reduce protein deposition on lenses [28, 29]. The application of biomaterials from other fields has advanced alternative manufacturing methods, allowing for more complex contact lens designs.

2.4.2 Current Manufacturing Practices

There are three main methods for manufacturing soft contact lenses. Lathe cutting was originally used to manufacture hard, soft and contact lenses. The process begins by filling rod shaped molds with a lens mixture solution of the desired monomers [4]. The rod is then placed in a controlled temperature bath to polymerize the rods. These polymerized rods are then removed from the mold and placed into a lathe to be cut into buttons, where the lenses are shaped to the desired size and base curve with a rapidly rotating cutting tool. While it is straightforward for rigid contact lenses, the swelling factor of the hydrogel material for soft contact lenses needs to be accounted for [4, 10]. Modern lathes cut with high precision and do not require polishing. This labour-intensive method of manufacturing is slightly outdated and difficult to scale so it is usually only used for complex lens designs or when developing a hybrid lenses [4, 10].

Spin casting was more common than lathe cutting as it was easier to mass produce lenses, whereby a liquid monomer mixture is added to a female mold and ultraviolet (UV) cured or heated to initiate polymerization while the mold is being spun [4, 10]. The mass of monomer injected, and the spin speed determined the geometry of the lens influencing key factors like the base curve and thickness of the central optical zone of the contact lenses [4, 10].

The most common method of producing lenses is cast molding, increasing in popularity due to the increased use of daily disposable CLs in the 1990's and its low cost per lens to manufacturers [4, 10]. It is similar to spin casting but simply uses a male and female mold to determine the lens geometry. The sandwiched molds are placed under UV light to initiate polymerization of the pre-polymer mixture and removed once hardened [4, 10]. This method of mass production produced high quality daily disposable CLs but is very limited when more complex lens designs might be required.

Current manufacturing trends point towards an increase in automation and improving current methods [4, 10]. However, with a growing shift in personalized medicine across a breadth of fields, there has been an increase in direct-to-consumer companies [10]. As such there's an interest in exploring high volume and flexible manufacturing processes, through a combination of currently methods or a more explorative approach like 3D printing (3DP) [10]. This method offers high customizability and quality thus may simplify the general process as polishing may not be needed but has limited throughput with the current technology available [10].

2.4.3 Bandage Contact Lenses

Bandage contact lenses (BCLs) are commonly prescribed for ocular surface diseases, traumatic corneal injury or recovery post-corrective surgeries, with the first being FDA approved in the 1970s [5, 31]. BCLs provide pain relief by acting as a protective barrier between the cornea and the external environment and eyelids which can irritate the cornea during wound healing. They also provide a scaffold for re-epithelialization while hydrating the corneal epithelium and enhancing corneal wound healing. BCLs also improve the tear film stability, corneal wound healing and maintain corneal hydration thus improving comfort for extended wear [5, 31].

As BCLs are typically worn for extended periods, SiHys are preferred due to their high oxygen permeability. This is needed to avoid corneal hypoxia, however, SiHys have poorer wettability due to their more hydrophobic nature [5, 31]. This can negatively impact the healing process as corneal hydration is reduced but the higher demand for oxygen during for corneal abrasions and the need for extended wear outweigh this issue. The fitting of lenses also impacts recovery depending on the patient's needs. In some cases a limbal or scleral lens that is slightly larger than the conventional BCLs are used [5, 6, 31]. Tighter fitting lenses minimize movement on the eye and disruption of the healing cornea, although, some lens movement can help promote healing. BCLs therefore generally have a steeper base curve to account for their larger size so they still fit tightly to the corneal surface while allowing some movement on the eye [5, 6, 31].

BCLs have their limitations and complications, particularly with discomfort and infection. Lenses generally disrupt the tear film, splitting it into the pre- and post- lens tear film, which is responsible for holding the lens to the corneal surface [5, 6, 31]. This results in a decrease in tear film stability and increase in evaporation rates leading to dryness which is further exacerbated by the hydrophobic nature of SiHy BCLs. These lenses are also prone to lipid deposition which can cause friction when blinking. New developments in SiHy CLs combat these problems by incorporating wetting agents or post-processing treatments, but have to be used in conjunction with lubricating and broad spectrum antibiotic drops in cases of extended wear [5, 6, 28, 31]. Without proper compliance to these regimens, CLs users are susceptible to biofilm formation and infection which can be detrimental during the wound healing process. Microbial keratitis is the most common infection CL users experience, caused by poor hygiene [5]. This is a general risk for contact lens wearers but can prove more problematic for BCL wearers following a traumatic ocular injury, with the wound at risk of being infected. SiHys are already prone to bacterial

adhesion due to their hydrophobic nature so compliance to these lubricating and antibiotic eye drop regimens and regular follow-ups are required to ensure an effective treatment plan [5, 6]. Compliance rates amongst eye drop users have been low since the 1990's at roughly 57%, whereby patients struggled with self-administration as most users are over 50 [3].

2.4.4 Drug Eluting Contact Lenses

There has been decades of research exploring the use of contact lenses as drug delivery systems to maintain therapeutic levels of drug on the eye while overcoming the issues associated with current ocular drug delivery practices, particularly the clearance mechanisms and various barriers of the eye [4, 26]. In an effort to increase the residence time and bioavailability of ocular therapeutics, therapeutic contact lenses (TCLs) have been examined as drug reservoirs. A common problem is the loading and release of therapeutic agents from the lens matrix generally results in burst releases which is undesirable for staying within the therapeutic window for a sustained period [32, 33].

Contact lenses have been shown to increase the residence time of a therapeutic agent and the cornea significantly compared to eye drops which have shown a corneal bioavailability of only 5% compared to 50% seen with TCLs [26, 33]. The CL divides the tear film, creating a post- and pre-lens tear film (POLTF and PLTF), with the former being in between the lens and the cornea [26, 34]. The therapeutic agent is released from the lens into both regions under a diffusion gradient, with the POLTF experiencing a slower clearance rate protected from the clearing mechanisms of the eye experienced by the PLTF and undisturbed film [34]. This allows for a much higher exposure time of the drug to the cornea, estimated to be about 30 mins compared to the 2-5 mins seen with eye drops [26, 34].

Various loading methods have been utilized to add therapeutic agents to CLs, with the most common being soaking [4, 26]. Here, the lens is immersed in a drug solution/suspension, with the drug steadily being absorbed into the lens polymer matrix through diffusion. The degree of drug loaded into the lens is positively correlated with the time immersed and the concentration of the solution [4, 26]. However, the amount absorbed by the lens is influenced by the lens material itself. The affinity of the drug to the lens is a major limitation and relies on numerous factors, including water content, lens thickness and drug molecular weight [4, 26, 33]. Poor and high affinity leads to low drug loading and/or burst releases of the therapeutic agent within a few hours or most of the drug being trapped within the polymer matrix, respectively [4, 26]. While soaking does allow for the drug's residence time with the cornea to increase, the burst or no release dilemma limits its applicability, especially for long term use [4, 26, 33].

Macroscopic approaches to loading lenses have been limited but also show a great deal of promise. These approaches have primarily been explored through drug-polymer embedded films, with the drug-polymer film being synthesized then placed in between a partially cured male and female lens mold that is then pressed and cured with the film [3, 4]. A study done by Ciolino et al. produced a poly(lactic-co-glycolic) acid (PLGA) film with either fluorescein and ciproflaxcin as the therapeutic agent achieved sustained release at near zero-order kinetics for over 100 and 28 days, respectively [3, 4]. These films showed incredible promise and tuneability as they could be used for multi-drug loading and release profiles could be altered based on the film thickness [3, 4]. A major drawback of the film is the lack of transparency despite the presence of a clear optic zone as this has been suggested to make the lenses aesthetically unappealing [3, 4]. Additionally, the manufacturing process of the drug-polymer film involves a three-day process and requires the use of a biopsy punch to manually create the clear aperture [35]. While progression of the inclusion of

the film into the lens has been made, it is still difficult to scale as the film needs to be synthesized separately and manually inserted to achieve this design [35].

Microscopic approaches to drug loading involve incorporating loaded nanocarriers (NCs) into CLs. These are commonly used in suspension formulations for eye drops and can greatly increase the residence time and minimize drug metabolism [4, 26, 36]. Thus, by incorporating NCs into lenses, you can create a compounded drug delivery system as the NC and CL both act as a diffusive barrier to further prolong the drug release rate [4, 26]. These NCs can take the form of nanoparticles (NPs), micelles, liposomes or microemulsions, generally, and can be loaded into CLs through various means. Adding loaded NPs or drug with a surfactant to the pre-monomer mixture are two methods of incorporating these nano structures into a lens, with the latter forming micelles as the surfactant aggregates around the drug [4, 37]. An alternative approach is implement the soaking method with a NP suspension to let the lens absorb the NPs into the polymer matrix. Additionally, NPs can be grafted or immobilized onto the lens surface which can offer another rate-limiting mechanism if the bond was degradative or responsive to certain stimuli like pH [4, 38]. However, like any approach, there are significant limitations to this, primarily the issue of NP aggregation that reduce lens transparency and the burst release seen while the lenses are stored, limiting their shelf life and applicability [4].

2.5 Vitamin E

A growing area of interest has been the incorporation of Vitamin E (VE) with a drug into the lens. VE has proven to be an effective diffusion barrier that can be incorporated into the polymer matrix of a lens and prolong the release of a desired therapeutic [4, 37, 38]. The impact of the VE barrier is dependent on the hydrophobicity of the therapeutic agent and the lens material itself as these can alter the release mechanism [4, 37, 38].

Vitamin E (VE) is a group of lipid-soluble compounds that are essential for antioxidant activity in the body, with a variety of sources like nuts, oils and leafy vegetables [7]. There are two naturally occurring forms of VE (Figure 4), tocopherols and tocotrienols, signified by their saturated and unsaturated hydrocarbon side chains, respectively, each with four variants in structure: alpha, beta, gamma and delta [7]. Alpha- tocopherol is the most prevalent in the body, found in the blood plasma and red blood cells, as the other forms get metabolized quicker [7]. This is due to the stereoselective nature of receptors and enzymes that enables only one enantiomer to bind while the other variants are metabolized and excreted [7].

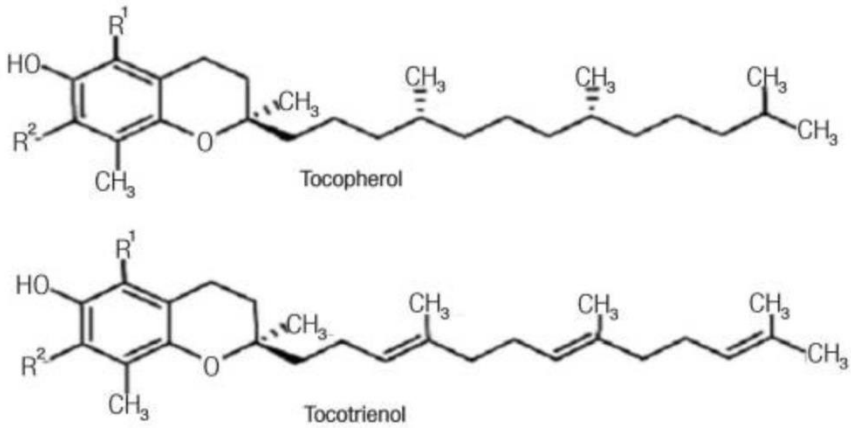

R^1	R^2	
CH_3	CH_3	α
CH_3	H	β
H	CH_3	γ
H	H	δ

Figure 4: Structures of the two classes of Vitamin E, tocopherol and tocotrienol, and the four variants of each molecule [7]

2.5.1 Vitamin E in Ophthalmology

VE is a powerful antioxidant that prevents the production of reactive oxygen species thus preventing free radical formation and can prevent or slow the progression of various health conditions [7]. Oxidative stress is linked to numerous diseases and conditions throughout the body, including: cancer, aging-related diseases and arthritis [7]. It also plays a role in various ocular disorders, including cataracts, age-related macular degeneration and glaucoma, making VE important to maintaining ocular health [7]. This has seen it used to prevent a host of age-related conditions and neurodegenerative diseases, including cataracts and age-related macular

degeneration (AMD). Cataracts occurs due to the buildup of proteins, damaged by free radicals, on the lens of the eye, leading to vision loss [7]. VE supplementation has shown promise in a few studies at slowing the progression of lens opacification due to its radical savaging properties [7]. A more severe neurodegenerative disease where the use of VE has been explored is for both forms of AMD [39]. Dry AMD is the more common form that is characterized by small deposits that cause the thinning and breakdown under the macula called drusen, leading to the loss in central vision [40]. Wet AMD is a more severe but rarer form whereby abnormal growth of fragile blood vessels underneath the macula leak blood and fluid into the region, resulting in a rapid decline in central vision [40]. VE has shown various pathways in which it can reduce the progression of intermediate and advanced AMD, with oxidative stress impacting photoreceptor cell death and inflammatory cytokines contributing to the progression of AMD [39]. VE's ability to inhibit oxidative stress plays a crucial role in the management of these ocular diseases and it has also gained traction in developing nanocarriers that can improve the efficacy of various ocular treatments [41].

2.5.2 Vitamin E Ocular Drug Delivery Systems

Vitamin E has been used in a variety of drug delivery systems for the eye, most notably D-alpha-tocopheryl polyethylene glycol 1000 succinate (TPGS) which has been FDA approved [41]. TPGS is a water-soluble Vitamin E co-polymer formed through the esterification of PEG and VE succinate, giving rise to an amphiphilic structure that is ideal for various drug delivery systems (DDS) [8, 41].

Most TPGS formulations have been nanocrystals/nanosuspensions where the copolymer acts as a surfactant to stabilize the system, which has shown to improve both the solubility and transcorneal permeability of the therapeutic agent [8, 41]. For example cyclosporine, an

immunosuppressant used for dry eye [41], was prepared as a micellar system of TPGS and Poloxamer showing enhanced drug loading and improved corneal and scleral permeability enabling delivery to posterior region through less invasive means [41]. Furthermore, TPGS has been used to develop an *in-situ* gel with Pluronic P123, a triblock amphiphilic copolymer, to improve the solubility and permeation of curcumin [41], used in ocular ointments and creams for the treatment of corneal wound healing, cataracts and glaucoma due to its anti-inflammatory and antioxidant properties [41]. *In vitro* release studies showed a sustained but limited release profile over 100 hours, likely due to the high affinity of curcumin for the copolymer gel and potential formation of micelles, limiting its release [41]. *Ex vivo* studies did show improved corneal permeation by a factor of 1.32, likely due to the depolymerized surfactants that are released as the *in-situ* gel degrades over-time. TPGS has also been used to develop PLGA (poly(lactic-co-glycolic) acid) nanoparticles that reduce the rapid clearance rate that limits ocular drug delivery [41]. Dexamethasone-loaded PLGA-TPGS nanoparticles intravitreally administered into rabbit eyes showed sustained release over 45 days with a constant release rate over the first 30 days compared to the 7 days it took to clear a regular dexamethasone dose [41]. Vitamin E-based DDS have been applied to a variety of areas outside of ocular therapeutics, including nanocarriers for treating multiple forms of cancer, prodrug formulations and improved entrapment efficiency of both hydrophilic or hydrophobic drugs due to its amphiphilic nature [41].

2.5.3 Vitamin E in Contact Lenses for Drug Delivery

VE has also been utilized in various studies as a diffusion barrier to either prolong the release of hydrophilic drugs or increase the retention of hydrophobic drugs [4, 9, 42]. In a majority of these studies, both VE and drug were incorporated via soaking and relying on the entrapment efficiency of the lens hydrogel matrix to control loading properties. A factor that heavily impacts

how much VE effects drug release is the lens material itself [9]. In silicone-based CLs, VE affinity has a positive correlation to water content, while the amount of VE loaded had a negative correlation with it. This could be due to more hydrophobic lenses being able to absorb more VE as it dissolves within the matrix and form aggregates rather than a barrier within the lens [9].

It was found that HEMA CLs co-loaded with VE and a hydrophilic drug used for glaucoma treatment, timolol maleate, had a minimal impact on the drug release profile but significantly improved loading [42]. Silicone lenses, on the other hand, showed significant increases in release duration, as a result of an increase in VE loading [9]. In ACUVUE Night & Day^{TM} lenses, an increase from 10% to 40% VE loading saw a rise in timolol release time from 5 to 400 h, respectively [9]. Similar results were seen with other hydrophilic drugs in SiHy lenses like dexamethasone phosphate and fluconazole which are used as an anti-inflammatory and antifungal drugs, respectively [9].

While VE incorporation in CLs has proven to be an effective means of prolonging the release of hydrophilic drugs, it can negatively impact lens properties [9]. The presence of only 10% VE has shown to slightly increase lens size while significantly decreasing oxygen and ion permeability by 40% and 50% respectively [9]. Furthermore, lens transparency issues have been reported when incorporating VE with varying results [9, 42]. Another limitation with current practices is the lens soaking method, whereby the lens material, loading solution concentration and contact time with the lens heavily influencing drug loading and release [4]. Many previous studies using this method have noted a significant initial burst release, with much of the drug remaining on the external surface rather than within the polymer matrix of the lens. Overall, VE incorporation into lenses improves the loading and release of therapeutic agents, depending on their affinity to VE but there are issues to be overcome. VE in free form can also acts as a secondary therapeutic

with its antioxidant and anti-inflammatory properties that could prove useful for traumatic corneal injuries [4]. Direct incorporation into the monomer mixture before polymerizing the lens could be a means of controlling VE loading and even drug loading to a much greater degree while also saving a great deal of time as lens soaking can lengthen the lens preparation process significantly.

2.6 Vat Polymerization Bioprinting

3D printing (3DP), also known as additive manufacturing, is the process of utilizing computer-aided design (CAD) to print materials in a layer by layer manner [13, 43]. Stereolithography was the first 3DP method invented by Charles Hull in the 1980s, where ultraviolet light was used to crosslink thin layers of material together to develop 3D structures [13]. Over the past few decades, 3DP has emerged in various industries, including the aviation, dental and automobile sectors for rapid prototyping and production of highly customizable parts [15, 43]. Interest in 3DP has increased in the healthcare sector, giving rise to 3D bioprinting, which refers to 3D printing of develop living and non-living biomaterials that can be used to develop functional tissues/organs, medical devices, pharmaceuticals, or surgical tools [11]. There are 3 main methods for 3D bioprinting: Vat polymerization (VP), extrusion-based and droplet-based printing with their characteristics described below in Table 1. VP has proven to be excellent for rapid prototyping with generally excellent surface quality and high print resolution [11, 44]. There are two main systems of vat polymerization. Stereolithography (SLA) utilizes a UV laser-assisted setup that cures in a point-by-point manner, resulting highly accurate but slow prints. Digital light processing (DLP) or masked SLA (MSLA) cure whole layers immediately allowing for fast build times but lower surface resolution; these typically operate with a visible light source rather than UV [44, 45]. The principle lies in using a light source to induce localized photopolymerization of

a resin, alternatively known as a bioink, to cure whole layers of a specified height of the desired object, allowing for fast and accurate prints [44, 45].

Table 1: Comparison of Primary 3D Bioprinting approaches [11]

Bioprinting Method	Principle	Speed	Cost	Resolution	Examples
Extrusion-based	Forms continuous filaments to form a layer	Slow	Medium	Medium	Fusion Deposition Modelling (FDM)
Droplet-based	Polymerizes across 2D plane in a point-by-point manner	Medium	Medium	High	Inkjet Laser-assisted
Vat Polymerization	Cures whole layers at once through photopolymerization	Fast	Low	High	Stereolithography (SLA) Digital Light Processing (DLP)

2.6.1 Formulation Components

Bioinks are solutions of natural or synthetic polymers that are biologically favourable for their intended purpose, with cell-free or cell-laden mixtures used to develop solid 3D structures used to develop biomaterials, living tissues or models [11, 44]. They consist of three main components: monomers, photoinitators and photoabsorbers or dyes [46]. A majority of these monomers are acrylates, like PEGDA, characterized by fast reactivity and oxygen inhibition that improves printability [46, 47]. There are drawbacks to acrylates as they tend to shrink when cured, however inclusion of methacrylates in the bioink reduce this [46], due to a slower curing rate and fewer reactive species present in the bioink, contributing to a slower curing rate and lower crosslinking density [44, 46, 47]. Acrylates generally have good printability but add a lot of rigidity to the final structure which is not ideal for soft biomaterials. Other common monomers include thiol-ene or epoxy systems that have their own benefits such as softer mechanical properties. VP also enables the inclusion of unreactive species as they can be functionalized with a reactive species like methacryloyl groups to provide photoreactivity [46]. There is therefore a wide variety

of monomers that can be incorporated to attain the physiochemical and mechanical properties desired, depending on the application. The formulation impacts printability factors like the viscosity and stiffness of the prints, with more reactive species resulting in faster photopolymerization [44, 46, 47] but very stiff prints as a result of many unreacted double bonds remain present within the 3D printed structure. Monomer molecular weight can impact printability significantly as low molecular weight monomers have lower viscosity and greater mobility whereas a higher molecular weight results in less shrinkage but increased rigidity and viscosity [47]. Viscosities for SLA printing ideally vary between 0.25 – 10 Pa s. High viscosity impacts VP printing as the print plate needs to recoat itself by rising and then falling back into the bioink in preparation of printing the next layer, resulting in longer print times [47]. PEG derivatives, particularly PEGDA is a very common monomer used in bioprinting with various molecular weights commercially available, allowing for a great deal of tuneability based on the biological application. Viscosity, hydrophilicity and the elastic modulus of prints with PEGDA are all positively correlated with its molecular weight and composition of the bioink [47]. The crosslinking density increases with higher ratios of PEGDA, resulting in stiffer structures. Thus, many bioinks used for soft tissues or biomaterials vary between 10-20% PEGDA as structures tend to become brittle beyond 20% [28, 47].

Photoinitiators (PIs) are essential to the VP process as they initiate the free radical photopolymerization process by absorbing light [44, 46, 47]. This creates a reactive radical species that then radicalizes the monomers to begin propagation; termination occurs when the light source turns off at the end of a printed layer. The emitted wavelength that the 3D printer uses should match or be close to the absorption wavelength of the PI to get optimal initiation. There is a wide variety of PIs based commercially available that work between 200-600nm, however, cell-laden

bioinks generally use PIs within the visible light spectrum to avoid potential UV damage to the seeded cells [44, 46, 47]. Additionally, the PI needs to show low cytotoxicity to prevent any cell apoptosis within the printed structure or during its use within any biological system. The limited number of PIs that meet these requirements is summarized in Table 2. SLA and DLP/MSLA printers work at 355nm and 405nm typically, respectively, so the latter is more commonly used in bioprinting [44, 46, 47]. Lithium phenyl-2,4,6-trimethylbenzoylphosphinate (LAP) is commonly used in bioprinting due to its higher water solubility and generally low cytotoxicity profile, making it easy to use in scaffolding for tissue engineering and hydrogel systems. It is a PI that is functional in the visible light range thus can be used at higher wavelengths that are not damaging to cells which is important for cell-laden bioinks.

Table 2: Summary of PI's commonly used in VP bioprinting [39]

Photo-initiators (PIs)	**Max absorption wavelength (nm)**	**Light Spectrum range**
FMN Riboflavin-based	267	UV
Irgacure 2959	275	UV
LAP	375	Vis
VA-086	385	Vis
Eosin Y	514	Vis

Photoabsorbers and dyes are commonly incorporated to improve the printing quality and resolution [44, 46, 47]. They limit the depth the light source penetrates through the resin or bioink to mitigate overcuring in all directions thus giving greater control over the polymerization process. This allows for the designed structure to match the theoretical dimensions specified in the CAD models. Selection of a photoabsorber is based on the printer wavelength with many photoabsorbers covering the 300-500nm wavelength range that all VP systems work within [44, 46, 47]. For printers operating at 405nm, dyes like Sudan I and Tartrazine are commonly used and can be incorporated at very low concentrations ranging between 0.5-4 wt % of the formulation. Yellow

food colouring is a cheap and accessible dye that contains tartrazine and is quite hydrophilic, making it ideal to incorporate into 3DP formulations [44, 46, 47]. While these dyes are ingestible at low concentrations, they may have carcinogenic effects when in excess and typically need to be removed after printing.

2.6.2 VP Applications

VP has been extensively studied for biomedical applications, particularly in tissue engineering, microfluidic devices and drug development [14, 44]. A majority of the work has been focused on tissue engineering due to the high resolution and complexity of the prints that VP can achieve in shorter print times compared to other 3DP techniques. The ability to control the surface topography and the design of each layer allows for creation of hierarchical structures, that mimic the microenvironments of the native tissue/organ like skin, cartilage or bone [14, 44]. These are typically made with PEGDA or gelatin methacrylate (GelMA) based formulations as they provide a good scaffold for cell adhesion and proliferation [11, 47]. Microfluidic (MF) devices have long been used as a cost effective means of replicating experiments for various biomedical purposes, including disease diagnosis and modelling, drug discovery, point-of-care testing and developing organ-on-a-chip models [48]. While most MF devices are made through molding, 3DP has slowly been revolutionizing the fabrication process allowing for the utilization of several materials and creation of intricate designs with the diverse choice of materials and high quality prints [44]. One drawback VP overcomes when compared to the alternatives is the smoother channels due to the higher surface finish it produces, however, the channel sizes are limited by the relatively low resolution in the z-direction.

3DP has also opened up a new avenue for drug development with the flexibility it provides. It enables a more personalized approach for tailoring medications to patient needs rather than the

generic “one-size-fits-all” approach commonly seen in the pharmaceutical industry [14, 44]. The freedom of design and rapid production of small batches seen with VP make it suitable for this point-of-care approach. The drug can either be directly incorporated in the formulation prior to printing or added through spray coating and solvent swelling in a drug solution [14]. The freedom of design also enables control over release kinetics by embedding pores or designs to tailor the release of a drug to match a patient’s dosing regimen. The most common use of VP in drug development is seen with microneedles [14]. The high printing resolution and reaction mechanisms allow for sharp needles to be produced with a wider variety of materials than seen with alternatives like FDM. Typically, 3DP would be used to create a negative mold to fabricate microneedles, however, VP allows for a direct, one-step process [14]. This customizability has also seen VP be utilized in oral drug delivery create tablets with tunable release through both pill design and the formulation [14]. One of the first studies to examine this created a disced-shaped paracetamol tablet and found that they could prolong the release by increasing the PEGDA concentration in the resin [49]. This study also found that increasing the surface area to volume ratio by introducing perforations into the tablet increased the release rate, highlighting the potential for tunable dosing with VP [49].

A benefit of utilizing VP to develop hydrogels and tissue scaffolds is the layer-by-layer printing process allows for multi-material prints (MMP) to be created [50]. MMPs allow for more complex hydrogels or tissue scaffolds to be created than current automated manufacturing methods cannot produce. They allow for the combination of different material properties and the ability to take advantage of their unique properties that can alter mechanical and surface properties. A few different techniques have been implemented to develop MMPs. The main method employed is switching the resin during the print for the desired region or layer [50]. The print is paused at a

specified layer to allow for the material switch, the print plate is cleaned to minimize cross contamination of the resins. The print is resumed for the desired layers before repeating the process and switching the material back to the original resin. Attempts have been made to automate the vat switching process however, the cleaning process between switching resins still requires significant time whether it was done automatically or manually [50]. This method has been applied to develop pills with multiple medications for the same medication, called polypills [50, 51]. Typical pills are manufactured through compacting homogenous powders of fixed strengths without room for flexibility with dosing based on a patient's needs. Using PEGDA, six formulations with different therapeutic drugs in each, allowing for a defined amount of each medicine to be dissolved without over-saturating a single formulation which would otherwise negatively impact printability. Another benefit to utilizing 3DP was the ability to control the dosing by sizing the segments differently, highlighting the freedom of design of this manufacturing process [50, 51].

2.6.3 VP in Ophthalmology

Interest in 3DP in ophthalmology has increased over the past decade, with most studies for have involving extrusion-based printers to produce corneal or retinal models using as they are more common in bioprinting [13, 15, 16]. The shear stress applied by the nozzle can influence cell viability, functionalities and morphological properties of the bioprinted models [13]. Recent advances with VP technology, particularly the resolution and printing times has seen its use steadily increase for ophthalmic bioprinting purposes. It has primarily been used to create ocular prosthesis or implants due to the smoother surface finish compared to alternatives [13, 16]. 3DP eye prosthesis can significantly reduce the invasiveness and manufacturing time which are generally made using an alginate mold and hand painted [15]. The process can be fully digitized

and automated using an optical coherence tomography scanner to create a 3D image of the anterior segment. A CAD file can be generated using this image to then 3D print an accurate and personalized prosthetic eye, with manufacturing times cut from 6 to 3 weeks [15]. Another benefit of automating the process is the patient's data is digitally stored, making replacement prostheses easier to fabricate compared to using an alginate mold each time.

A similar approach can be taken to produce contact lenses to create more customized and better fitting CLs for patients. 3DP opens up the possibility of producing a variety of complex CLs, including smart and personalized therapeutic CLs that are limited by current manufacturing practices. Clear dental resin was recently used to create 3DP CLs using a DLP printer [17]. These lenses could be printed with microchannels and patterns without compromising the structural integrity of the lens greatly which could prove useful for adding biosensors to develop smart CLs. Another study utilized a PEGDA/HEMA blend and two different dyes to develop a multi-material CL that aids colour blindness correction [52]. They printed flat discs and localized one dye to the peripheral of the lens and the other to the center to help filter multiple wavelengths of light.

There have not been many studies ocular DDS fabricated via 3DP, however, they have mainly been done using FDM printers to create therapeutic patches that sit under the eyelid or CLs [43, 53]. A hydrogel patch consisting of hydroxylpropyl methylcellulose (HPMC), mannitol and xylitol with levofloxacin as the therapeutic agent [53]. Increased concentrations of mannitol and xylitol reduced the porosity of the patches which lead to a more sustained release of levofloxacin, although, no change was seen with mannitol. The tuneability of these patches was further exemplified with patches of different surface to volume ratios being fabricated which allows for control over the release rate of the desired therapeutic agent [53]. An FDM printed CL loaded with timolol maleate was made using a ethylene vinyl acetate (EVA) and poly (lactic acid) (PLA)

monomer blend [54]. The lenses were relatively clear as the printer had a slow print speed, however, ridges between the layers were visible. Additionally, a bulk of the drug was released within 5 h and there was only a slight increase in the timolol maleate released after the first day, likely due to poor diffusion of the drug through the polymer matrix [54]. The print quality of the loaded CLs was lower compared to the blank lens due to the poor miscibility of the drug with the bioink resulting in inconsistencies between print layers. The prints were also slow as a result of the low print speed needed to achieve a high resolution through FDM printing [54].

Punctal plugs manufactured using a DLP printer have shown a lot of promise for 3DP ocular DDS. The plugs were made of either a PEGDA or PEGDA/PEG400 formulation, loaded with dexamethasone (DEX) [43, 55]. Release studies showed a sustained release of DEX over 21 and 7 days, respectively, which was expected with the addition of PEG making the lens matrix more hydrophilic. While the release was quicker, roughly 100% of the DEX was released from the PEGDA/PEG400 formulation compared to the 60% seen with the PEGDA bioink. The higher crosslinking density of the PEGDA formulation and the poor aqueous solubility of DEX are attributed to the lower release with more of the drug being trapped within the lens matrix [43, 55].

Overall, the use of VP in ophthalmology has great potential as the high printing resolution and fast printing speeds would allow for on-demand fabrication of treatments tailored to a patient's needs [14, 16, 43]. The freedom of design that comes with 3DP enables complex designs to be utilized that can be used to tune the dosing regimen accordingly by increasing or decreasing the surface to volume ratio of the drug carrier. Dosing can also be managed directly by directly incorporating the drug in the bioresin prior to fabrication [14, 16, 43]. While there is a lot of promise with 3DP and VP in pharmaceutical and biomaterial manufacturing, there are limitations to it. In particular, the small batch production volumes cannot meet the output that current mass

production process have which will likely lead to an increase in manufacturing costs [14, 16, 43]. However, the incorporation of 3DP into healthcare can be fully maximized by limiting its focus to unique or specialty treatments that require a more personalized approach.

In this work, 3D printing methods were examined with a goal of creating drug delivering bandage contact lenses with the potential to better treat patients post corneal wounding.

3.0 Materials and Methods

3.1 Materials

Poly (ethylene glycol) diacrylate (PEGDA) (Mw = 700g/mol), hydroxyethyl (methacrylate) (HEMA), ethylene glycol dimethacrylate (EGDMA), lithium phenyl (2,4,6-trimethylbenzoyl) phosphinate (LAP), anhydrous tetrahydrofuran (THF), triethylamine (TEA), methacrylol chloride (MAC), dichloromethane (DCM) and chloroform-D and (+) δ-tocopherol (Vitamin E) were all purchased from Sigma Aldrich (Oakville, ON, Canada). Silica particles (mesh size 40-63µm) were purchased from Silicycle (Quebec, ON, Canada). Methacryloxypropyltris (trimethylsiloxy) silane (TRIS) was purchased from Gelest (Pennsilvania, US). Club House yellow food dye was purchased through Amazon. MilliQ Water was prepared in-lab with a Milli-pore Barnstead water purification system. Phosphate buffered saline (PBS) was prepared in-lab by dissolving 8.5g of sodium chloride, 0.345g of monobasic sodium phosphate and 1.32g of dibasic sodium phosphate in 1L MilliQ Water before being adjusted to a pH of 7.4. Dexamethasone phosphate was the gift of Eyegate Pharmaceuticals (Boston, MA) and stored in MilliQ Water at a concentration of 40 mg/mL.

3.2 Methacrylated Vitamin E (VEMA) Synthesis and Preparation

3.2.1 VEMA Synthesis

Since the reagents in VEMA synthesis are highly reactive and sensitive to moisture and light, glass was scrubbed and cleaned with sparkline soap, then dried in an oven (70°C).

In a fume hood, 5g of (+) δ-Tocopherol was dissolved in 75 mL of THF in a round-bottom flask (RBF). Once homogenous, 4.35mL of TEA was added. The flask was purged with nitrogen,

secured closed with a septum, sealed with parafilm, and placed in an ice bath for one hour. 1.5ml of MAC was gradually added into the RBF through the septum using a needle and syringe. The RBF was left covered with aluminum foil to react in an ice bath for 4h then at room temperature overnight, while stirred 600 rpm.

3.2.2 VEMA Separation and Purification

Following reaction, vacuum filtration was performed to remove precipitated TEA salt. The filtrate underwent rotary evaporation, at 100-150 rpm at 30-40°C until no THF passed through the condenser into the receiving flask, indicating all of the THF had been extracted. The unpurified VEMA was then resuspended with approximately 5-10 mL THF and filtered before rotovapping again.

After this, column chromatography was performed to remove any other impurities including unreacted reagents or side products. The column was prepared by making a 1:2 w/w% mixture of silica particles to dichloromethane (DCM). After the silica gel had settled in the column, a thin layer of sand was spread evenly to protect the top silica layer as DCM was repeatedly added to the column.

Before beginning column chromatography, thin layer chromatography (TLC) was done using the unpurified VEMA to create a reference. TLC allowed for comparison of extracted column samples, collected in test tubes, to identify impurities and to assess what sample range purified VEMA is within. Unpurified VEMA was then poured into the column. Once the top layer of the product had passed through the silica, DCM was added into the column and sample collection began. DCM was continuously added to prevent the silica from drying out. TLC was performed for each fraction, and the TLC plates were viewed with a UV lamp to identify which

samples contained the purified product. Purified fractions that only showed a single dot on the TLCs were collected. The purified VEMA underwent rotary evaporation to remove the remaining DCM. The VEMA was then transferred into a 20 mL vial, weighed before being stored at -20^{o}C until use.

3.3 Bioink Preparation and 3D Printing Parameters

3.3.1 Bioink Preparation

All bioinks were prepared in round bottom flasks (~100mL for each batch). The hydrophilic and hydrophobic components of the bioinks were prepared separately before combining to improve the miscibility of all components. PEGDA was weighed, placed in a 50 mL beaker and left to become a viscous liquid at room temperature. The photoiniator (PI) solution was prepared by steadily dissolving 600 mg of LAP in 10 mL of PBS. This PI solution was then added to the PEGDA and covered by aluminum foil due to its UV sensitivity. Yellow dye was added to this mixture and left to stir for 1 h. HEMA and EGDMA were added directly to the RBF and left to mix for 0.5-1 h. VEMA or VEMA and TRIS were then added to the HEMA/EGMDA mixture at this step depending on the formulation being prepared. After sufficient mixing, the PEGDA/PI mixture was added to the RBF and left to mix for another hour. All formulations were stored refrigerated at 4^{o}C. The drug-loaded batches were prepared by dissolving dexamethasone phosphate (DXP) directly into the bioinks at a concentration of 12.71 mg DXP/g bioink. The composition of each of the formulations is shown in Table 3 below.

Table 3: Composition of the three bioinks shown by a weight/weight percentage (w/w %)

w/w (%)	HEMA	PEGDA	EGDMA	DYE	LAP (in 10ml PBS)	VEMA	TRIS
Base	65	20	2	3	0.6	-	-
+ VEMA	60	20	2	3	0.6	5	-
+ TRIS + VEMA	45	20	2	3	0.6	5	15

3.3.2 Single and Multi-Material Lens Design

The single and multi-material lens designs were developed using Autodesk Fusion360. The lenses were designed to be discs, 14 mm in diameter and with theoretical thickness of 300 – 600µm. For the multi-material lenses, a ring insert was embedded with a 7mm gap in the centre to create a clear optical zone and 200 µm depth. The CAD files are converted to Standard Triangle Language (.stl) format that is commonly used for slicing software. Chitubox was used as the slicing software and to set the printing parameters. This software slices the 3D object across the z-axis based on the layer height defined and then converts the file to a readable .zip file for the 3D printer.

3.3.3 3D Printing and Printing Parameters

The lenses were fabricated using the Anycubic Photon Mono X (Shenzhen, China) with a 4k resolution LCD screen that utilized DLP or MSLA printing. To prepare the actual model lenses, the vat was first filled with the desired bioink and the appropriate lens design was loaded. For single material prints, the prints occurred without interruption until completion. For multi-material prints, the prints were paused at the appropriate layer, such as during the manufacturing of the embedded ring. The print plate was cleaned without removing the cured discs to prevent cross contamination of the different bioinks and to minimize material loss. The printing resumed with the different bioinks until the ring was complete and previous step repeated to complete the print. Once the prints were complete, the print plate was detached and cleaned. The printed lenses were

removed carefully from the print plate to prevent damage. Samples were then soaked in MilliQ Water to remove the dye. The printing parameters set in Chitubox are listed in Table 4. The printer operateed on a two stage motor control allowing for faster prints while maintaining print quality and resolution.

Table 4: 3D Printing parameters for lenses

Printing Parameter	**Specifications**
Layer Height	0.05mm
Exposure Time	45sec
Lift Distance	5mm
Lift Speed	130mm/min
Retraction Speed	144mm/min

3.4 Material Characterization

3.4.1 H-NMR Sample Preparation

For characterization of VEMA, H-NMR was used. Approximately 5-10 mg of the VEMA sample was placed into a disposable 5 mL glass vial with 1 mL of chloroform-D. After mixing, the sample was transferred into a clean NMR tube using a glass pipette, until approximately a quarter of the tube had been filled. H-NMR analysis was performed using Bruker NEO600 machine at the McMaster University NMR Facility. All results were analyzed using Bruker's TopSpin program.

3.4.2 Bioink Absorbance and Lens Transparency

The absorbance of the bioinks were measured by placing 50 µL samples of each bioink in a 96-well VWR sterile tissue culture plate and diluted with 150µL of MilliQ water. The well plate was then placed into UV-VIS spectrometer and the absorbance of the bioinks is measured through the 300-800nm range.

Optical transparency of the model lenses was determined using light transmittance (T) of fully hydrated lenses. The model lenses (n=3) were placed in a 12-well VWR sterile tissue culture plate with 3 mL of MilliQ water. The absorbance was measured using a UV-VIS spectrometer BioTek Cytation 7 Cell Imaging Multimode Reader (Aligent Technologies Inc., Mississauga, ON, Canada) over the 380-800 nm range. The measured absorbance of the lenses was then subtracted from a reference sample of just MilliQ water and converted to transmittance using the equation below:

$$T\ (\%) = \ 10^{(2-Absorbance)} \quad (1)$$

3.4.3 Viscosity of Bioinks

The viscosity of the bioinks was measured by rheometry (Discovery HR-2 Hybrid Rheometer (DHR) with TRIOS software by TA Instruments). A 40mm 1^{o} cone plate was used to measure the viscosity and deformation profile of the formulations. Once the cone plate had been zeroed, the cone plate was raised to loading height and a 400 µL sample of the desired bioink was placed onto the peltier plate while ensuring no bubbles were present. The cone plate was lowered and then a flow sweep analysis of viscous and flow behaviour was conducted at 25^{o}C. The TRIOS software produces a plot of shear rate vs. viscosity and shear stress to highlight the viscosity and flow profiles.

3.4.4 FTIR

To determine lens surface chemistry, ATR Fourier Transform Infrared Spectroscopy (FTIR) was performed. The lenses were dried in the vacuum oven for 12-24 hours prior to checking the lens. A Nicolet 6700 Fourier Transform Infrared Spectrometer (Thermo Scientific, Waltham, Massachusetts USA) was used to measure the absorption spectra in the range of 600- 4000cm^{-1} (64 scans, 4 cm^{-1} resolution). The ATR crystal was lowered until sufficient contact with the lens was made (n=3). Different contact points across the lens surface were assessed to create an average for each sample that was measured.

3.4.5 Model Lens Imaging

TEM images of the model lenses were produced to view the uniformity of the hydrogel matrix within the lenses. Discs were printing using each bioink and left to soak in water overnight to remove the yellow dye. The hydrated model lenses were then placed in a vacuum oven at room temperature for 12-24 h to dry. TEM was run on each of the discs. Thin sections (90 nm) of each lens were cut on a Leica UCT ultramicrotome and picked up onto Cu grids. The grids were viewed in a JEOL JEM 1200 EX TEMSCAN transmission electron microscope (JEOL, Peabody, MA, USA) operating at an accelerating voltage of 80 kV. Images were acquired with an AMT 4-megapixel digital camera (Advanced Microscopy Techniques, Woburn, MA).

Images of the lens were also obtained using a dissection and stereo microscope to observe the macroscopic structure of the multi-material 3D printed lenses. Samples were printed and left to dry overnight before being placed under the on the microscope stage for the images to be acquired.

3.4.6 Contact Angle

Surface wettability of hydrogel surfaces was measured using sessile drop contact angles. Water contact angles were measured using Model 100 NRL Goniometer (Rame-Hart Inc., New Jersey, USA) on fully hydrated lenses. Excess water was removed from the surface of the lenses using a Kimwipe®. A single 10 µL drop would be placed on the lens surface. The contact angle was measured by observing a tangential line from the point of contact between the drop and the hydrogel surface through a light microscope setup. All measurements were completed at ambient temperature and humidity (n=3).

3.4.7 Water Content

To assess the water content of the model contact lenses, the lenses were swollen in MilliQ water for 48 hours. The lenses were carefully blotted with a KimWipe to remove excess water and the mass determined. The lenses were placed in a vacuum oven to dry for 24 hours and then weighed to determine mass change (n=3). The water content was calculated using the formula below:

$$Water\ Content\ (\%) = \frac{Final\ Wet\ weight - Initial\ Dry\ weight}{Final\ Wet\ Weight} \quad (2)$$

3.4.8 Mechanical Testing

Mechanical testing was carried out using a benchtop universal mechanical testing system, Instron Model 3366 (Instron Corporation; Norwood, MA), following ASTM D638 standards in order to measure the modulus, tensile strength and extension of the various formulations. Sheets (<1 mm) of each formulation were printed and cut out using the designated dog-bone mold. The samples were the soaked in MilliQ Water overnight. The average thickness of each sample is

measured using a micrometer. The samples are then dried using a Kim Wipe and placed in between clamps with minimal tension. The test is then ran following the ASTM D638 method until the samples tear and the process is repeated with the remaining samples.

3.5 Drug Release

The loaded formulations were sonicated to ensure the DxP was fully dissolved. A low loading concentration was used to minimize potential printing issues. Triplicate sets of blank and loaded single material lenses were printed for the release studies. The lenses were briefly rinsed with MilliQ Water after printing and dried with a KimWipe before being weighed to determine the amount of drug per lens. The lenses were then left to soak in 500 µL of PBS in a 24 well-plate overnight. The lenses were then dried and placed into Falcon tubes with 5mL of fresh PBS. The Falcon tubes were placed into an incubated shaker plate for the release study. Samples were collected periodically at specified time points with the release media refreshed each time. Calibration curves were prepared using a stock solution of 5 mg/mL of DxP, appropriately diluted, in PBS. All samples were analyzed using the Aligent 1260 Infinity II high performance liquid chromatography (HPLC) (Aligent Technologies Inc., Mississauga, ON, Canada).

4.0 Results and Discussion

4.1 VE Methacrylation

Following the method of Jianfang et al. [56], methacrylated VE (VEMA) was synthesized to create a photocurable vitamin E (VE) that can be directly crosslinked with the hydrogel matrix of the lens, with the schematic shown in Figure 5. The hydroxyl group from the delta-tocopherol reacts with the carbonyl carbon from the methacryloyl chloride (MAC) in a nucleophilic attack that expels the chlorine from the MAC. The hydroxyl is then deprotonated and the hydrogen bonds with the chlorine ion to form hydrochloric acid as a byproduct, leaving VEMA as the final product. Triethylamine (TEA) was used as a catalyst in this reaction but also neutralizes the hydrochloric acid produced, forming a TEA salt as a byproduct of the methacrylation process.

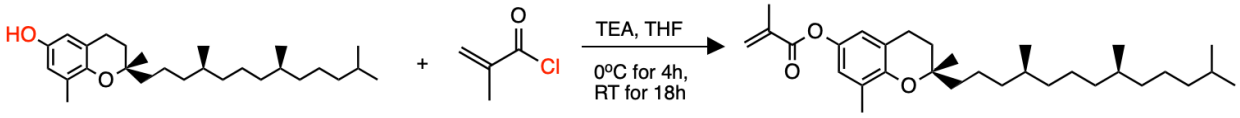

Figure 5: Methacrylation reaction of Vitamin E to synthesize a photopolymerizable Vitamin E for the modified print formulations

The ^{1}H-NMR demonstrating successful methacrylation of VE is shown in Figure 6. It can be seen that the peaks at 6.61 and 6.68 (e, f) correspond to the benzyl ring from the VE group and peaks at 5.65 and 6.27 (h, g) correspond to the carbon double bond from the methacrylate group. ^{1}H-NMR The ratio of the integrated peaks was used to assess the purity of the collected VEMA following the TLC column, as shown in Figure 6, with a ratio close to 1:1 suggesting little to no reactants remained in the final product, following purification through the silica column.

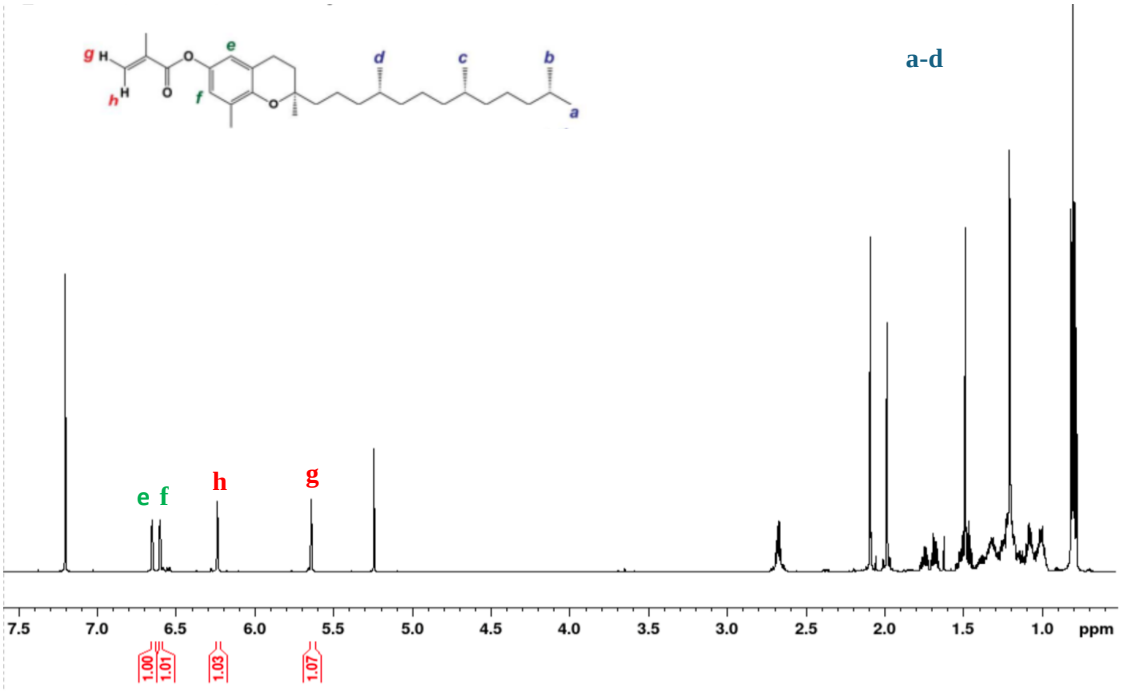

Figure 6: H-NMR spectrum of methacrylated Vitamin E with chloroform-d as the solvent, with a solvent peak seen at 7.24. The hydrogen peaks of the methacryloyl chloride are highlighted by the h and g letters and the hydrogens on the delta-tocopherol are highlighted by the letters e and f. The integrals of the peaks are shown below the x-axis, with the 'e' peak used as the reference for the others.

4.2 Bioink Characteristics

A flow sweep analysis was conducted to assess the rheological properties of the bioinks used in these studies as this can impact the printing quality and speed. Figure 7A and B suggest that the bioinks showed a shear thinning profile with a viscosity that decreased with an increase in the shear rate. The addition of VEMA or TRIS did not significantly impact the viscosity as PEGDA and HEMA make up the bulk of the formulations. Shear thinning inks with low viscosity are ideal for vat polymerization (VP) as the print plate requires minimal force to break the surface tension of the liquid and spreads more quickly and uniformly over the print plate, allowing for quicker print times as less time is needed between layers to properly recoat the print plate. These bioink characteristics are likely due to the low molecular weight of the components used.

The absorption profiles shown in Figure 7C were assessed to examine their printability with the printer that operates at a wavelength of 405 nm. Figure 7C shows all bioinks have a peak ranging 350-450 nm which is associated with the yellow dye. The dye is added as a photoabsorber to improve the printing resolution by minimizing light scattering and penetration to achieve prints as close to the theoretical dimensions as possible. The early peak seen at approximately 320nm followed by a rapid decline before rising again at 340nm is characteristic of the LAP photoinitator which has a peak ranging from 340-415nm that overlaps with the yellow dye. The overlaps in peaks likely causes the double peak seen between 400-450nm in all formulations, with a minor dip at around 410nm. Overall, the yellow dye and formulation have an absorption range that suits the operating wavelength of the printer of 405nm to minimize issues that could impact the printing resolution such as overcuring and light scattering.

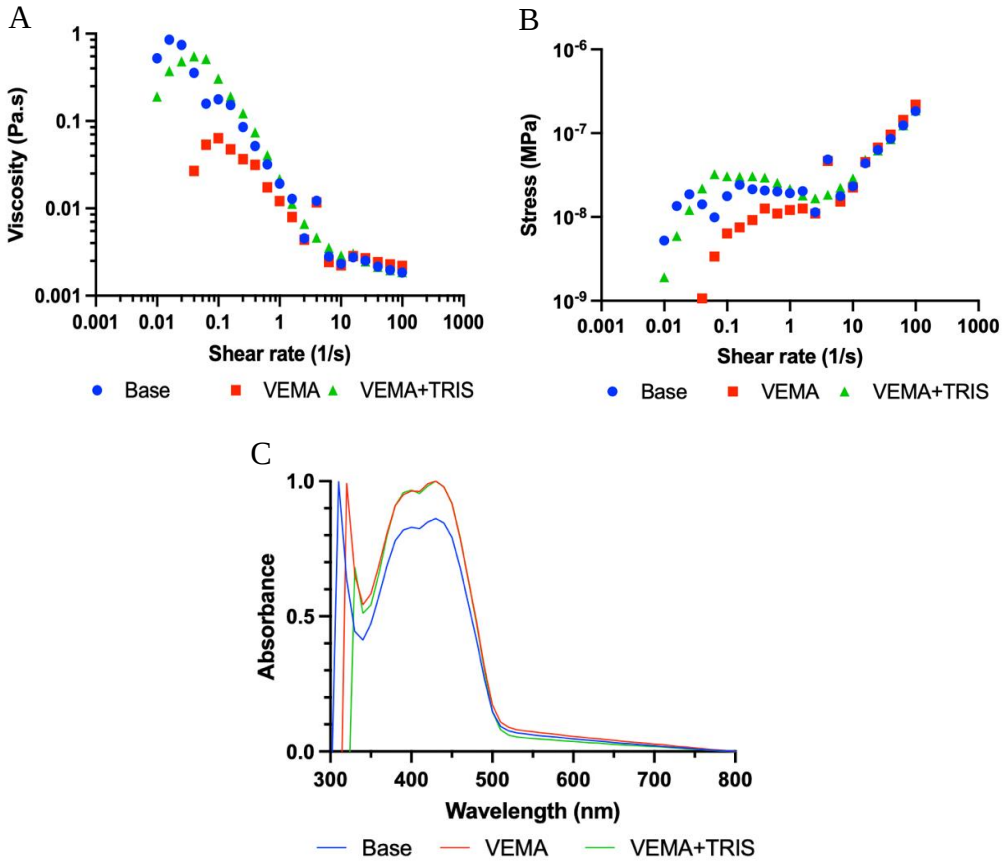

Figure 7: Overview of bioink characteristics of the three formulations. Flow sweep analysis conducted to show the Viscosity (A) and Stress (B) under shear stress to determine how the bioinks flow during 3DP. The Absorbance (C) of the bioinks assessed over the visible light range (300-800nm) to determine photoabsorption abilities at the printer's operating wavelength (405nm)

4.3 Lens Design and Manufacturing

4.3.1 Lens Designs

Two simple lens designs were developed using a CAD software to create the single and multi-material (MM) lenses, shown in Figure 8A and B, respectively. The discs were designed with a diameter of 14 mm and a theoretical thickness of either 300 µm or 600 µm. The MM lenses included a 100 µm thick ring embedded between two flat discs, with a clear optic zone of 7mm to minimize the effect the drug-loaded ring on the overall transparency of the lens. The MM design also enables a relatively simple printing approach whereby the prints can be paused to swap

materials before and after the ring layers. Furthermore, the clear optic zone is filled in when printing the top layers as the resin fills in the void as the start of the top layer is cured.

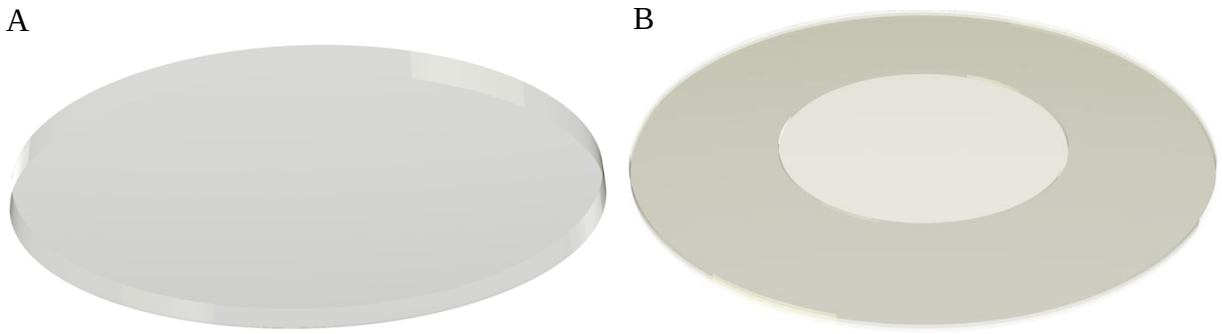

Figure 8: CAD Designs of the single (A) and MM (B) lens design with 14mm diameters and thicknesses of either 300 or 600µm. The MM lens has an embedded ring at the peripheral of the lens with a 7mm width and a clear optic zone in the center

4.3.2 Printing Accuracy

The accuracy of the printer was assessed by comparing the CAD and actual discs printed for both single and multi-material lens designs. The results are shown in Table 5. Single material discs with a theoretical thickness of 300 µm and 600 µm, were printed to determine if the discrepancy between theoretical and printed discs increased with a thicker sample.

Table 5: Discrepancy in lens thickness between the CAD design and printed discs (n=3)

Design	**Thickness (µm)**	
	Theoretical	**Actual**
Single material	600	824.33 ± 117
	300	544.43 ± 72.84
Multi-material	300	551.11± 51.29

The actual thickness of these samples were 544 ± 72.84µm and 824 ± 117µm, respectively, suggesting there is a degree of overcuring or inaccuracy. The 600µm and 300µm discs were printed with a defined layer height of 50µm, giving each a total of 12 and 6 layers. However, based on the layer count, the layer height seen with the 600µm and 300µm, the actual layer height seen is

roughly 69µm and 90µm, respectively. The thicker prints show a higher degree of precision likely due to the error discrepancies between layers being minimized with a higher layer count. Reducing the layer height could minimize the discrepancy between the theoretical and actual models as the layer count would increase and create more precise prints, however, this would also significantly increase the print times with more layers to cure. The MM prints indicate that the change in design and material had a negligible effect as the lens thickness achieved was the same as the 300µm disc.

The formulation also is also a contributing factor as the printer's layer height and z-resolution are typically based on the company's own unique formulations which is likely to vary for non-conventional 3DP formulations. The formulations used primarily consisted of reactive species with PEGDA, EGMDA, HEMA, VEMA and TRIS all containing at least one acrylate group, which could contribute to the overcuring seen. While the viscosity of the print mixture was well within an acceptable range, reducing the monomer concentration or adding a diluent could reduce the crosslinking density and minimize overcuring. Another factor is the photoinitiator (PI) concentration as this can impact the print speed, crosslinking density, and cure depth. All formulations used a PI concentration of 0.6% (w/v) of LAP which is close to the recommended range 0.25-0.5% for bioprinting with a DLP printer [47]. A higher concentration was used primarily because the printer operates at the 405nm wavelength which is at the tail-end of LAP's max absorption peak at 375nm [44]. The exposure time can also impact overcuring; however, the 40-45 s range was the necessary exposure time to achieve consistent prints that would adhere to the build plate. The improvement in printing accuracy with thicker samples can be attributed to the effects of the yellow dye that limits light penetration for thicker prints. Thicker discs require deeper light penetration through the formulation to cure the bottom layers as a print continues. This is due to the fact that the light intensity decreases as it passes through the solution or

component containing the yellow dye, which acts as a photoabsorber, limiting light penetration [47]. This limits the impact of overcuring of the bottom layers in thicker prints thus improving the accuracy as well. Overall, further optimization of the formulation is required to achieve more accurate prints that minimize overcuring without sacrificing print speeds. Utilizing smaller layer heights could be explored to create more accurate prints while identifying the ideal exposure time that correlates with thinner layers to minimize the increase in print time.

4.3.3 Print Quality

TEM imaging was performed to examine the morphological properties of the single material discs to observe how the addition of VEMA and TRIS impacted the disc and print quality. The results are shown in Figure 9. The base formulation, which primarily consisted of PEGDA and HEMA, showed a very homogenous print, suggesting good miscibility between the components of the formulation. However, the addition of VEMA significantly impacted the print quality with the presence of numerous defects, likely due to the poor miscibility between the hydrophilic components and VEMA. The poor miscibility can be seen clearly at the 800nm scale, with distinct regions of separation, depicted as a mix of dark and light sections. The formulation appeared homogenous prior to printing, however, a combination of the agitation from the print plate and poor miscibility is believed to create air pockets, resulting in the large pores seen in the VEMA prints.

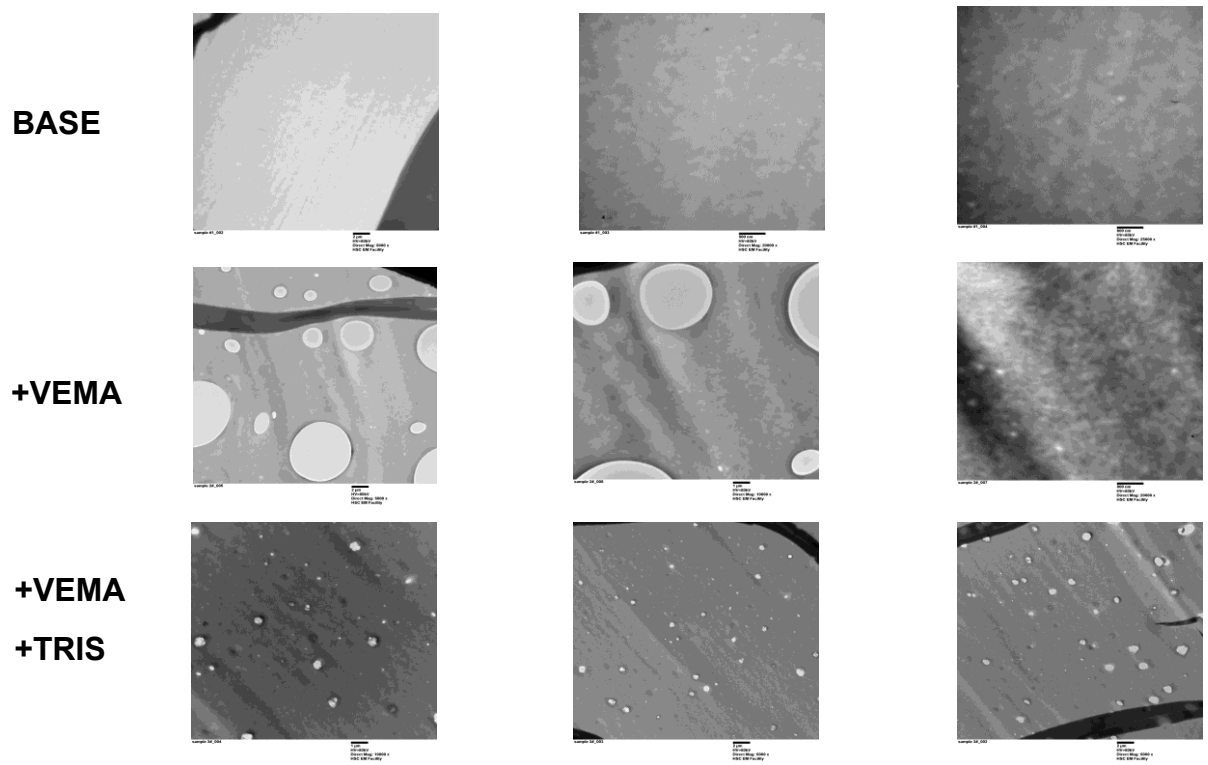

Figure 9: TEM images of the Base, VEMA and VEMA+TRIS printed lenses to observe changes in morphology to examine the impact of the modifications to the base formulation on the print quality

The VEMA+TRIS prints showed a significant improvement to the initial modification, with increased homogeneity and a lower number of defects. The prints appeared much more uniform while the pore size decreased significantly compared to the VEMA prints. This shows that TRIS improves the miscibility between the hydrophobic and hydrophilic components of the formulations. The hydrophobic interaction between the siloxy groups of TRIS and the carbon chain of VEMA presumably helped to stabilize VEMA within the PEGDA/HEMA phase. The flexibility of the TRIS side chains is also believed to reduce steric hinderance with the bulky VEMA molecules, allowing for better dispersion and uniformity within the formulation. TRIS itself has a good balance between hydrophilic and hydrophobic moieties between the methacrylate group and trisiloxy side chains, allowing for good miscibility of other hydrophilic and hydrophobic moieties.

This allowed for a more stable polymer network, resulting in more consistency in the quality of the model lenses produced through DLP printing.

4.3.4 Multi-Material Prints

Multi-material (MM) prints were developed to examine the potential freedom of design that 3DP has to offer by embedding a drug loaded polymer ring within a lens directly. Previous attempts with this have involved a partially cured female and male part of a CL being pressed and cured together following manual insertion a polymer ring in the female mold prior to curing [3]. This manual approach limits scalability and leaves room for error in placing the polymer ring in the correct spot consistently while a 3DP approach automates this process.

The VEMA formulation was chosen for the embedded ring as the cure times for the base and VEMA formulations were similar, making the transition periods simpler to design and print, as seen in Figure 10A. The VEMA+TRIS formulation was not tested for MM prints as initial exposure times per layer for the formulation were 100-110 secs compared to 40-45 secs for the other formulations, making switching back to the base material difficult without overcuring. While the VEMA+TRIS formulation was eventually optimized to have a 40-45 s exposure time, it was not tested for MM printing. A clear boundary between the embedded ring and clear optic zone can be seen in Figure 10B. A lattice pattern can be seen when looking at the center Figure 10B, which is a result of the LCD screen pixels which imprint this grid-like structure throughout the print which could have an impact on the lens transparency. Furthermore, while the screen does have a 4k resolution, the rapid advancement of 3DP technology has seen the development of printers with 9k and 12k resolutions presently which could improve the transparency of the prints.

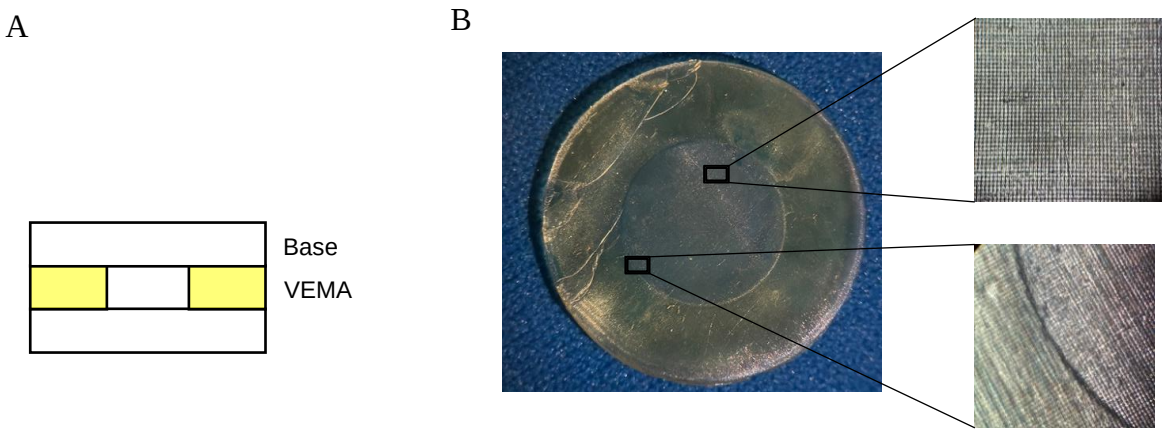

Figure 10: (A) Cross-sectional diagram of the MM lens design with a VEMA ring surrounded by a top and bottom layer of the Base material. (B) Light microscopy image of the MM lens to clearly show the boundary between the clear optic zone and VEMA ring

Table 6 shows the discrepancy seen between the center and edge of the MM lens, which is roughly 50-70 µm or one layer. This discrepancy is due to the need for the center to be filled while the top layer is being cured, leaving a void in the center for the optic zone while the ring is being printed. As such the base material fills this void while the top layer of the lens is being cured and is progressively filled. However, as the print begins from where the ring layers end, the top base layer has the foundation of the ring to build upon on the edge while having to fill the void. While the difference is not significant, the discrepancy did impact wettability as the center was obscured by the edge and impacted contact angle measurements. This discrepancy could be overcome by intentional overcuring to level the center and edge, as shown by *Hisham et al.* [52]. They used a cure time four times longer than the normal cure time to induce overcuring and create a uniform surface. While no overcuring was intentionally induced in this study, there was no statistically significant difference noted while a difference could physically be felt by hand ($p>0.05$). The eyelid is quite sensitive and it is believed that the difference would be felt, resulting in discomfort. Slight overcuring of the top layer could result in a more even center. Increases from 45sec to 50-60sec could lead to a more even surface. The size of the optic zone could be further optimized as a smaller void could be filled and cured easier.

Table 6: Multi-material lens discrepancy between the center and edge (n=3)

Center	Edge
488.44 ± 53.02	551.11 ± 51.29

Figure 11 shows TEM images of the center, boundary and edge regions of the MM lens to assess the print quality and the consistency of the prints through the material switch. As expected, the center was quite homogenous throughout. The striations seen are from the direction the samples were cut and the large breaks are simply from the resin used to cure the samples before cutting for TEM analysis. The boundary layer again mostly shows a uniform mixture, however, small aggregates can be seen which is likely the inner edge of the embedded VEMA ring. The aggregates could be attributed to uncured residuals of the VEMA ring mixing and polymerizing with the base formulation as it fills the void and is cured. The edge shows a mix of features between the base and VEMA prints seen in Figure 11, where there are homogenous regions and then more defective/porous regions that are similar to what was seen with VEMA prints.

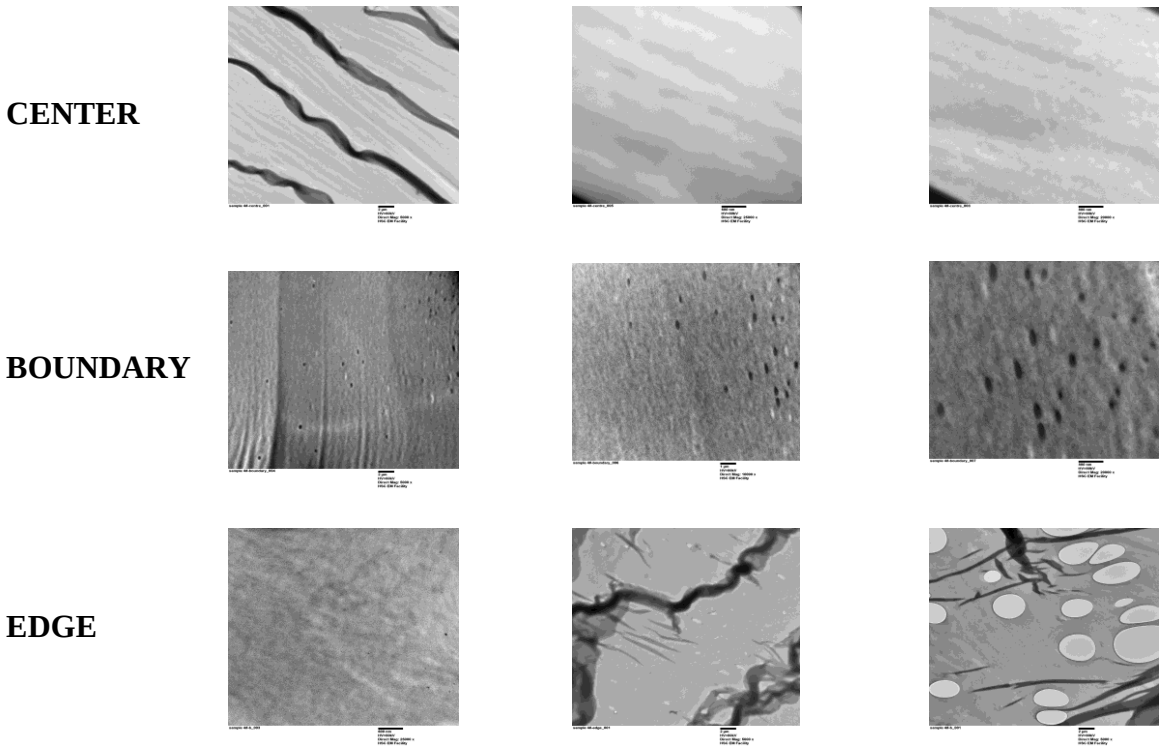

Figure 11: TEM images of the MM lens to examine the change in morphology across the different regions. The center is the optic zone, the boundary is the intersection between the optic zone and VEMA ring while the edge examines the peripheral of the lens which consists of the VEMA ring in between the base material

4.4 Lens Characterization

4.4.1 Surface Composition

ATR-FTIR was conducted to analyze the lens surface chemistry for the various modifications. The lenses were vacuum dried for 24 h prior to testing to remove any water as it can impact readings. The absorbance readings shown in Figure 12 are normalized.

As shown in Figure 12, the addition of the hydrophobic moieties and reduced concentration of HEMA in the modified formulations can be seen to lead to decreasing intensity between 3000-3600 cm^{-1} associated with hydroxyl (O-H) groups. The change in intensity seen at the 2750-3000 cm^{-1} range, associated with (C-H) can further supports the inclusion of the hydrophobic moieties in the modified lenses. There was an increase in intensity from the base to the VEMA lenses, due

to the aromatic and aliphatic C-H bonds on the VEMA molecules. There was a slight decrease in this with the addition of TRIS, as the concentration of HEMA was decreased in this formulation due to the presence of fewer C-H bonds present on TRIS molecules.

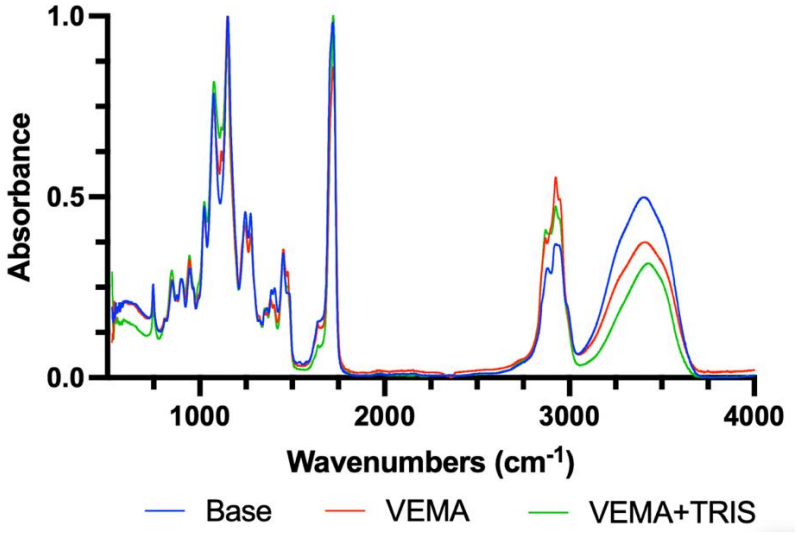

Figure 12: ATR-FTIR of the base and modified single material lenses to analyze changes in the lens surface chemistry (n=3)

There was a great deal of overlapping of peaks in the 500-2000 cm^{-1} range, however, changes in intensity of peaks can indicate key characteristics. It is worth noting the decrease in absorbance in the VEMA+TRIS lens at the 500-1000 cm^{-1} range associated with siloxanes (Si-O-Si) and C-H bending. This could suggest TRIS is altering the polymer structure with a more rigid/organized polymer network that can lower the vibrational activity. This can be seen again in the 1700-1720 cm^{-1} region associated with carbonyl groups (C=O) is lower/dampened in the VEMA+TRIS lenses. This change in structure could lead significant changes in physical properties and a more rigid material. While ATR only measures a few microns into the surface of a material, the use of a single formulation and using the average of three contact points from a single sample allow us to assume the composition is uniform in the bulk of the lens as well. Additionally, ATR-FTIR requires minimal sample preparation where the printed lens could simply be examined as in

a dehydrated state, whereas, a regular FTIR sample requires more complex sample preparation. Overall, the ATR-FTIR shows clear indicators of VEMA and TRIS being successfully incorporated can be seen in the modified formulations with potential impacts on structural and physical properties noted as well.

4.4.2 Hydrophobicity of Single Material Prints

The hydrophobicity of the single material lenses were assessed by examining the equilibrium water content (EWC) (Figure 13A) and contact angle (Figure 13B) of the prints. The water content is a useful guide to the bulk material properties of the hydrogel network that effect its water uptake while the contact angle allows for assessment of the surface wettability of the printed discs. Both properties are important for contact lenses as they affect comfort and handling while also impacting drug dissolution and release properties. There is a significant difference ($p < 0.05$) following the addition of VEMA and TRIS, decreasing the WC from 71.31 ± 2.17% for the base formulation to 64.41 ± 0.9% and 54.79 ± 1.32% for the VEMA and VEMA+TRIS formulations, respectively. This is the expected trend following the addition of hydrophobic moieties like VEMA and TRIS, along with a reduced concentration of the hydrophilic monomer HEMA for both formulations. The same trend can be seen regarding the contact angle, with a significant ($p<0.05$) increase from 41.3 ± 4.04^o to 75.67 ± 5.13^o between the base and VEMA+TRIS formulations. The VEMA formulation showed a slight but insignificant increase ($p > 0.05$) in contact angle compared to the base formulations from 41.3 ± 4.04^o to 57.67 ± 10.41^o, likely due to the low 5 w/w% VEMA concentration in the formulation.

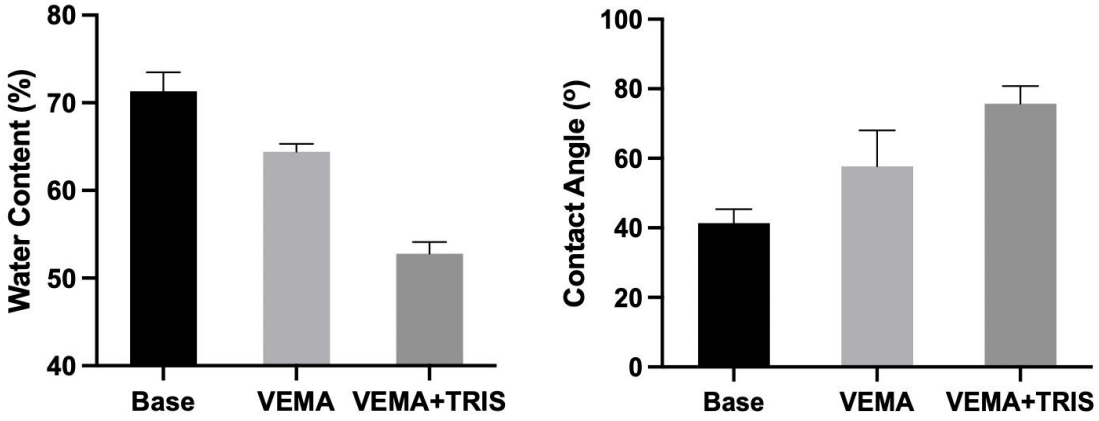

Figure 13: Equilibrium Water Content (A) and Contact Angle (B) to assess the hydrophobicity of the single material prints (n=3)

Compared to commercial standards, the EWC is quite high for all formulations, due to the inclusion of PEGDA. EWC of HEMA containing lenses can vary between 30-80%, suggesting that the printed lenses are within commercial standards [57]. While a high water content allows the lens to be fairly flexible and soft, it can also discomfort overtime due to the loss of moisture to the environment and reliance on tears for rehydration leading to dryness and irritation [57, 58]. For HEMA-based lenses, the EWC also impacts oxygen permeability whereby the higher the water content leads to greater permeability [28, 57]. However, in SiHy lenses, oxygen permeability is more dependent on the silicone content within the lens [28, 57]. The combination of PEGDA and TRIS monomers in VEMA+TRIS formulation result in a lens with a relatively high water content and high contact angle. The significant increase in contact angle could be attributed to the nature of the very mobile silicone-oxygen bonds that find their way to the surface of the lens [30, 59]. Thus, while these lenses may have an improved oxygen permeability and dehydrate more slowly, the surface wettability is poor which can affect the stability of the tear film over the lens [28, 57]. This was a common issue with first-generation SiHys prior to surface treatments being implemented [30, 59]. Another factor that can impact the contact angle of the lenses is the smoothness of the print plate surface. A rougher print plate enables better adherence of prints but

can impact the resolution as the plate pattern or roughness is imprinted throughout the layers of the printed object. While that can be attributed to the high contact angles compared to commercial standards, it is negligible regarding the difference in contact angles between the three formulations as the same build plate was used throughout.

4.4.3 Mechanical Properties of Single and Multi-Material Prints

The tensile mechanical properties of the lenses were assessed following ASTM D638 standards, normally used for industry, as they impact comfort and handling of contact lenses. Lenses with high moduli are easier to handle and have better eye movement but can be quite uncomfortable and cause a host of issues including corneal staining and superficial lesions [57, 60]. As such a balance between the two is ideal. Currently, most CLs available have low modulus ranging from 0.8-0.33 MPa, with a few higher modulus lenses ranging between 1-1.9 MPa [57, 58, 60]. Tensile testing was done on the single and multi-material prints to examine how the formulations and print quality impact the tensile properties as shown in Figure 14.

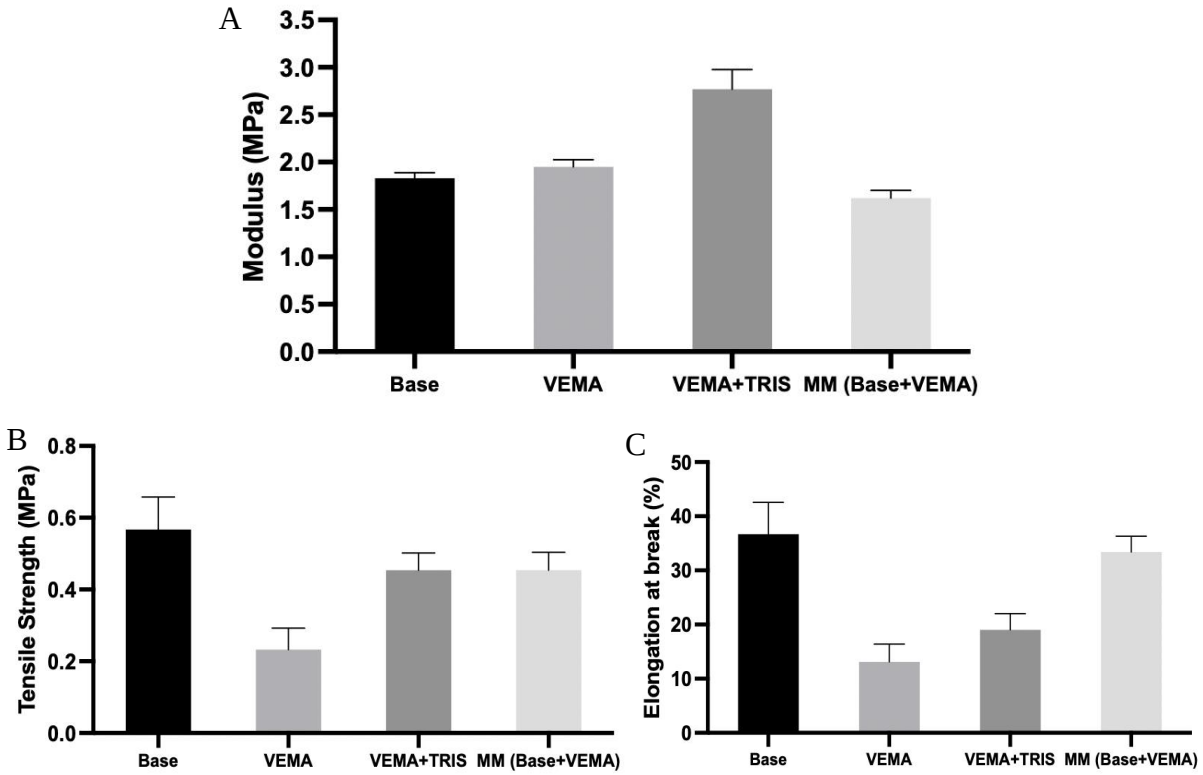

Figure 14: Tensile Properties of the Base, VEMA, VEMA+TRIS and MM prints highlighted by the Modulus (A), Tensile Strength (B) and Elongation at break (C) (n=6, 7, 7, 9, respectively)

Figure 14A shows the modulus of the single and multi-material prints. The modulus is defined as the longitudinal stress divided by the strain which are highlighted by Figure 14B and C,

respectively. All materials exhibited high moduli exceeding commercial standards, ranging from 1.62-2.77MPa, likely due to the high degree of physical entanglement of the PEGDA and HEMA chains within the hydrogel matrix. The addition of VEMA led to a slight but insignificant ($p > 0.05$) increase to the modulus compared to the base material. However, it had a significantly lower tensile strength and elongation profile compared to the base material. This can be attributed to the poor print quality and homogeneity of the VEMA lenses seen in Figure 9, making the material comparatively weak and brittle. The VEMA+TRIS formulation showed a significant increase in the modulus compared to both base and VEMA formulations with a modulus of 2.77MPa. This is a result of a significant increase ($p < 0.05$) in tensile strength compared to the VEMA formulation from 0.232 ± 0.06 to 0.454 ± 0.048 MPa with only a marginal increase in the elongation profile. This is partially due to the improved the miscibility between the hydrophilic and hydrophobic components with the addition of TRIS, resulting in improved printability. As TRIS is a hydrophobic monomer, the material has worse swelling properties as seen in Figure 13A, thus giving rise to a stiffer material.

The modulus of the MM prints is the lowest of the four groups at 1.62 ± 0.0827 MPa, where the tensile strength and the elongation profile are significantly better than the VEMA prints but slightly worse compared to the base material. This shows the MM lenses have a blend of tensile properties between the base and VEMA materials but predominantly favours base material properties. This favourability shows that the design of the MM lens also helps mitigate the poor tensile properties of VEMA material while reducing the stiffness of the lens compared to the base material. This suggests that the lens design could allow for monomers alternative to VEMA and TRIS can be incorporated into the ring without significantly impacting the overall mechanical properties of the lens.

4.4.4 3DP vs. Cast Materials

A comparison study of the tensile properties between 3DP and mold casting method, commonly used in CL manufacturing was performed, to examine whether the different methods of preparation impacted the mechanical properties. The test was conducted using the base material, As seen in Figure 15A, there is a significant increase ($p < 0.05$) in the modulus between the 3DP and cast material, jumping from 1.83 ± 0.0571 MPa to 2.42 ± 0.154 MPa.

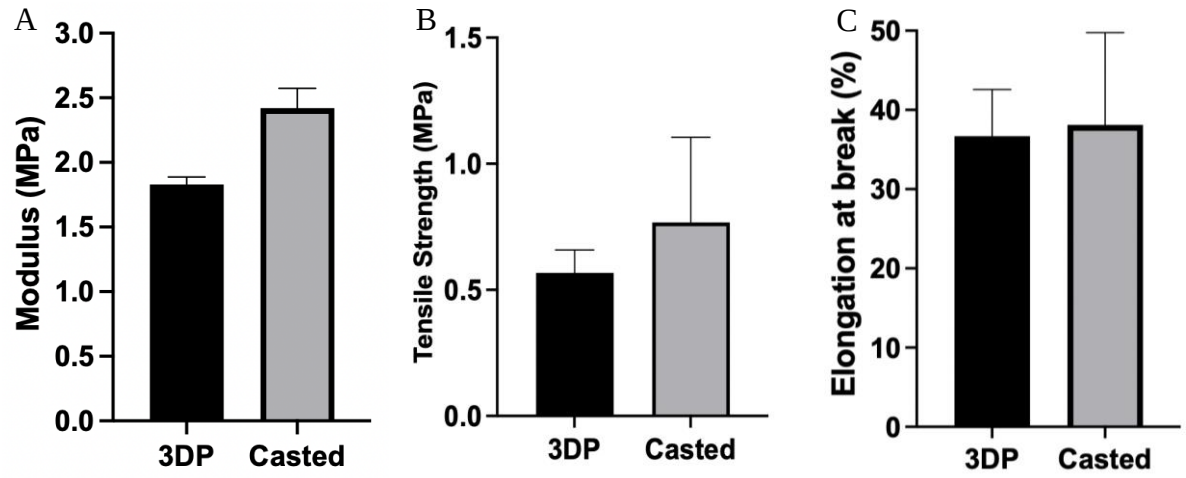

Figure 15: Comparison of the tensile properties of the base material after 3DP and Mould Casting summarized by the Modulus (A), Tensile Strength (B) and Elongation at break (C) to assess the impact of different manufacturing methods (n=6)

The higher tensile strength (Figure 15B) and similar elongation profile (Figure 15C) suggest that the 3DP lenses are stiffer than the cast material. This is likely due to the method of polymerization between VP and casting, where the latter involves uniform bulk polymerization while the former is in a layer-by-layer manner. 3DP objects are generally more fragile compared to cast materials as the layer-by-layer polymerization process leaves breaks between the layers. They also tend to have an uneven curing density within a single layer due to varying light intensity at different depths as a layer is polymerized. Bulk polymerization on the other hand is uniform throughout, with no separation of layers seen, creating a more structurally sound object. While casting does produce the stronger material, the 3DP modulus is closer to commercial standards for

CLs [57, 60]. General improvements could be made to the formulation to reduce the high modulus including reducing the monomer content and diluting the formulation. Additionally, removing monomers like EGDMA could reduce the modulus as EDGMA is commonly used as a secondary crosslinker in HEMA lenses, and may not be needed given the low concentration used and presence of PEGDA in the formulation.

4.4.5 Optical Transparency

Lens transparency is one of the key parameters behind CL design. Lenses ideally have a transparency >90% within the visible light range [28]. The material selection can reduce transparency if there is poor miscibility between the hydrophilic and hydrophobic components. The product quality is also impacted by the applied manufacturing method, as seen in this study, which can influence the transparency of the CLs as well [28].

The lenses were printed and soaked in MilliQ water for 24 h to remove the yellow dye as it impacts absorption readings between the 350-500nm range. As seen in Figure 16, none of the lenses meet commercial standard. Out of the single material prints, the base lenses performed the best while the VEMA and VEMA+TRIS formulations were significantly worse. This can be attributed to both the poor miscibility between the hydrophilic and hydrophobic components seen in the TEM images in Figure 9 and the low print quality seen with the modified formulations. Despite performing the best, the transparency of the base material only ranged between 80-88%. While the TEM images show a very homogenous lens, the transparency is still lower than commercial lenses. The VEMA and VEMA+TRIS prints showed a significant decrease in transparency, ranging between 18-47%. Despite the improved print quality seen with VEMA+TRIS prints, the transparency is slightly worse than the VEMA prints which can be attributed to the defects contributing to increased light scattering resulting in reduced transparency.

The MM prints with the VEMA ring show promise as there is a significant improvement in transparency compared to the lone VEMA prints and performs similarly to the base prints with its transparency ranging from 62-85%. Further optimization of the ring size and clear optic zone could improve this as well as exploring alternative materials for the ring itself.

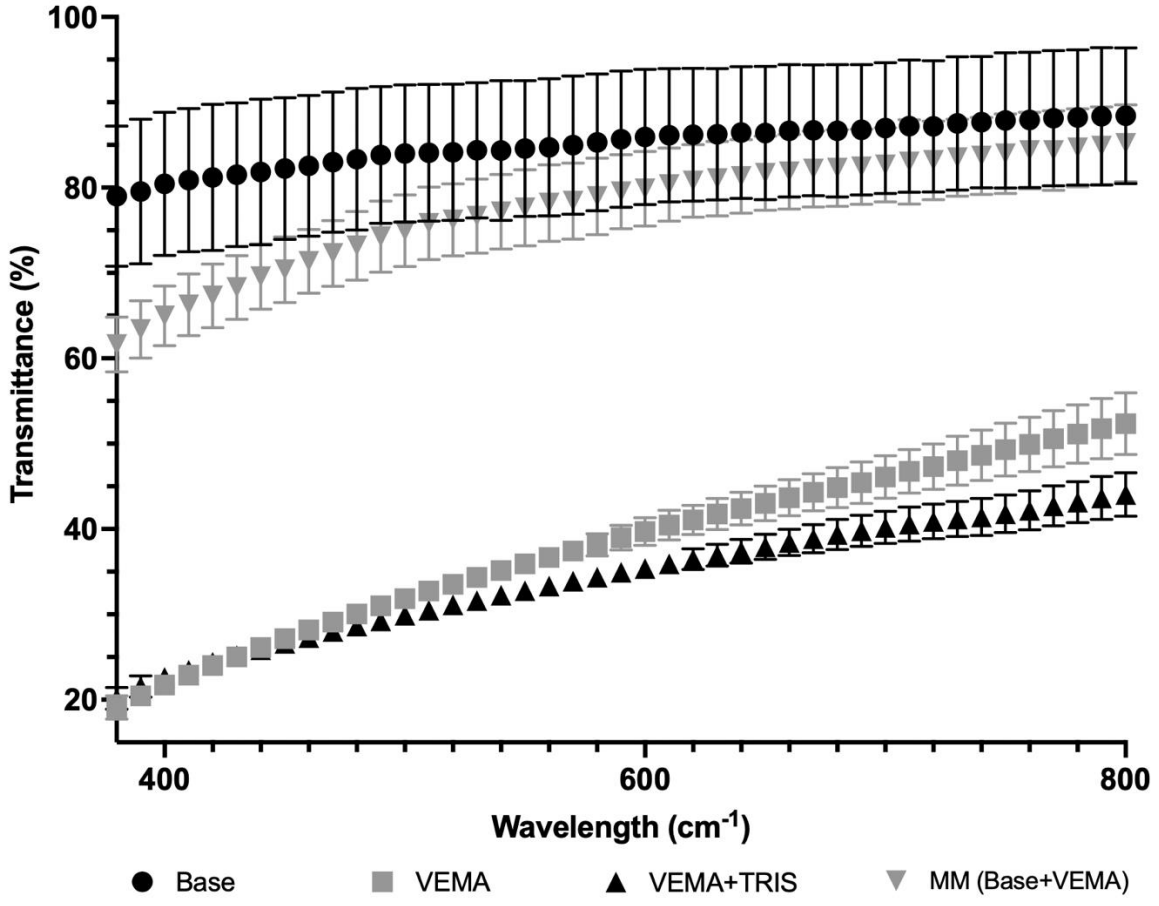

Figure 16: Transmittance of single and MM prints to assess how material composition and lens design can impact transparency over the visible light range (350-800nm) (n=3)

The printer resolution and print plate can have an impact on this as the print quality is affected by the screen resolution and pixel size that masks the light source to selectively cure the desired object. The print plate roughness impacts all layers and the surface of the lens as its impression is carried through all layers as they are cured. To further improve transparency, the

print plate can be made smoother although this can reduce adhesion of prints to the build plate. The printer used has a screen resolution of 3840x2400 which provides a 4K resolution. With the rapid growth in 3DP technology, newer printers with 6K and 9K resolutions have emerged and could provide higher quality prints [61]. The lenses were also 500-600 µm thick which is significantly thicker than commercial lenses, a factor which also impacts transparency as the degree of light scattering increases with thicker lenses. Overall, further optimization is required to improve the transparency of the lenses to meet commercial standards, although, the MM lens design is able to mitigate the negative physical properties of the poorer print materials as seen in Figure 16.

4.4.6 Single Material Drug Release

A drug release study was conducted to see how different material composition of the prints would affect the release of a therapeutic agent. Dexamethasone phosphate is a hydrophilic derivative of dexamethasone, a corticosteroid that is as an anti-inflammatory agent used following corneal injuries. While it slows down the healing process, it mitigates aggressive inflammatory responses during the wound healing process, which is essential to prevent corneal scarring following trauma to the region as a result of chemical or physical injuries.

This study was performed to see if the lenses could be effectively loaded by directly mixing the drug in the formulation at 12.71 mg drug/g lens material. This concentration was chosen to minimize the impact that drug could have on the 3DP process as it can affect mechanical properties of the lenses. Directly manufacturing the lenses with the drug pre-loaded can also mitigate problems of dimensional changes seen with lens soaking which can affect lens fitting [9]. Additionally, a large amount of drug was required for each study; the volume required per batch of bioink was roughly 70-80 mL due to the vat size. As seen in Figure 17, the initial loaded amount

prior to the drug release study was roughly 0.9-1mg of DXP per lens in each group. The aim was to match a low daily dose of DXP for adults of about 0.75mg/day, administered 4-6 times throughout the day via eye drops [62-64]. However, an error was made where the lenses were soaked in MilliQ water overnight rather than a 1mg/mL DXP solution thus leading to a 50% release of DXP before the start of the study. As such, the lenses had roughly 400-500 ug at the start of the study and the cumulative release values are based on those values.

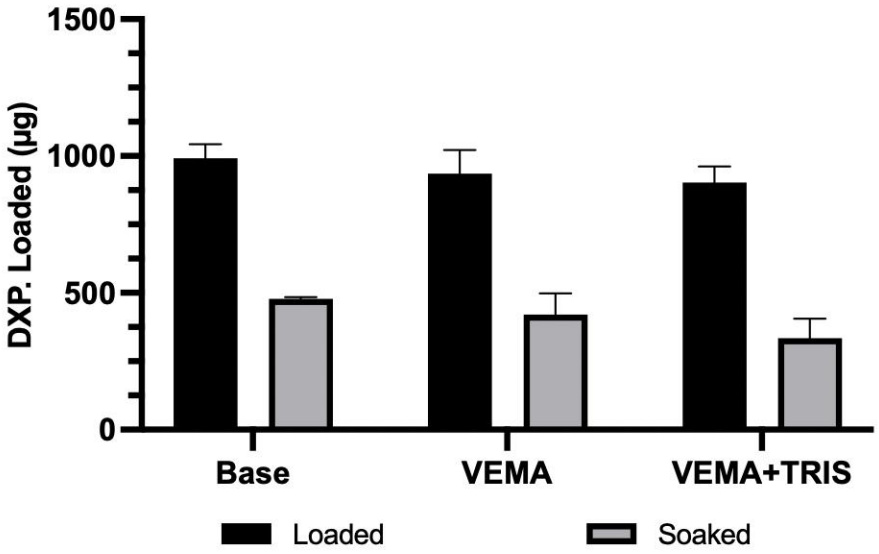

Figure 17: Average concentration of DXP loaded into single material lenses before and after overnight soaking in PBS solution (n=3)

The introduction of VEMA appears to slightly reduce the rate of release, albeit insignificantly as there is a minor reduction in the burst release as shown in Figure 18, with only 37.09 ± 4.81% being cumulatively released compared to the 44.09 ± 4.63% from the base lenses. Generally lenses with a higher water content can retain more of a hydrophilic drug but that also means that the drug has a higher affinity to the polymer matrix [32]. The drug is also more likely to be evenly dispersed throughout the lens matrix, allowing for a more gradual release. The phase separation seen in the TEM images in Figure 9 show the barrier that slightly reduced rate of release

seen in the VEMA prints, although a higher VEMA concentration is likely needed to see a significant effect.

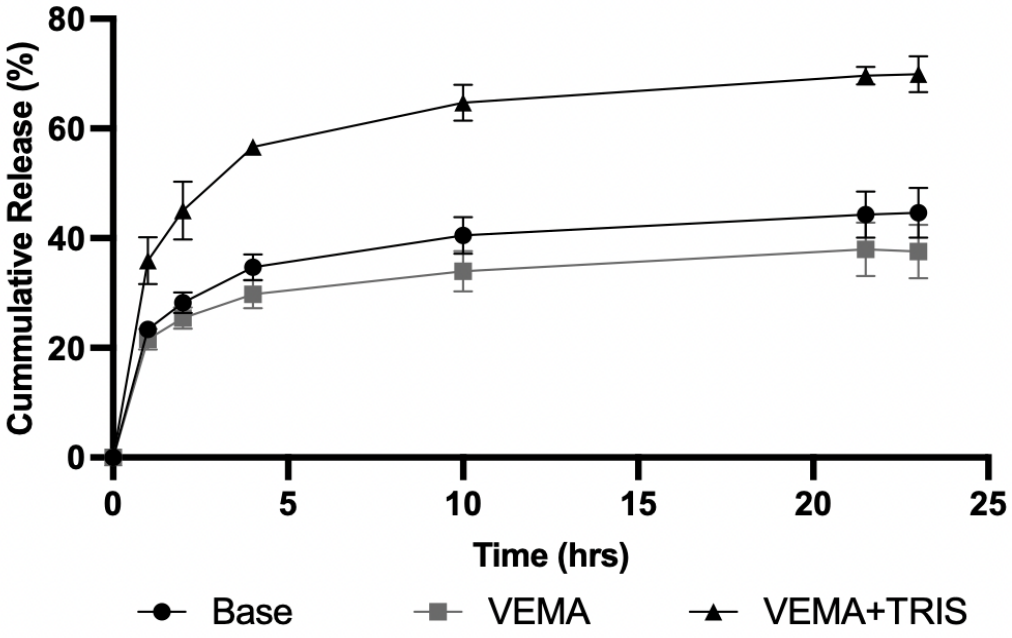

Figure 18: Cumulative release profiles of DXP from single material lenses over 24hrs. Lenses were soaked in PBS at room temperature for the period of this study (n=3)

The VEMA+TRIS lenses show a significant increase in the amount released from the lens compared to the Base and VEMA lenses, with 69.21 ± 3.62%, 44.09 ± 4.63% and 37.09 ± 4.81% being release released, respectively. This can likely be attributed to the more mobile silicone-oxygen bonds that are not as rigid as the carbon-carbon bonds that are seen with a majority of the components in the formulation. While this allows for increased oxygen permeability, it creates larger hydrophobic pores that reduce the degree of physical entrapment of DXP within the polymer matrix which could explain the significant difference in the amount released from the other formulations. Additionally, the hydrophilic DXP has a weak affinity towards the hydrophobic TRIS resulting in a rapid burst release with over 50% of the drug being released within 4 h. This high rate of release suggests that there is no apparent VEMA barrier that prolongs the release of

DXP. The improved miscibility of VEMA with the hydrophilic components as a result of adding TRIS also seem to mitigate its barrier effect at low VEMA concentrations.

The incomplete release of DXP from all lenses is likely due the error in sample preparation while swelling the lenses, leading to a significant amount removed and relying on a calculated estimate of the remainder in the lens at the beginning of the study. Other contributing factors that could influence this include the high degree of crosslinking within the lens polymer matrix, creating very small pore sizes which may contribute to high levels of physical entrapment. Another possibility is that some DXP reacted with the acrylate components of the lens formulations as the photopolymerization process creates free radicals which could lead to the formation of covalent bonds of DXP with one of the monomers in the formulation. Further optimization can be done by reducing the monomer concentration in the formulation while identifying ideal VEMA and TRIS concentrations in the modified formulations to achieve the barrier effect without compromising print quality.

A study by *Peng et al.* shows how the increased loading of Vitamin E (VE) via soaking into various SiHy's can impact various properties, including EWC and the release of hydrophilic drugs [9]. It was observed that loading higher concentrations of VE would prolong the release of various hydrophilic drugs including DXP. However, the effect of VE was dependent on the SiHy's composition, with a significant barrier effect observed with Acuve® OASYS™ where EWC decreased as more VE was loaded into the lenses [9]. PureVision™ lenses showed the same downward trend in EWC as the Acuve® OASYS™ lenses but no significant change in release was observed suggesting that the VE simply dissolved into the lens matrix [9]. NIGHT&DAY™ and O_2OPTIX™ showed reduced rates of release but not as significantly as Acuve® OASYS™ with the change in rate being attributed to VE aggregates forming rather than a barrier [9]

The difference in mechanism is attributed to the change in EWC seen with increased VE loading whereby the change is initially downward until a critical concentration whereby the VE no longer solubilizes in the gel matrix and shows a phase separation [9]. The Acuve® OASYS^{TM} and PureVision^{TM} lenses have a continuous downward trend where large amounts of VE are solubilized or coat the polymer fibers [9]. The difference in the effect of VE loading on the two lenses can be explained by this where the Acuve® OASYS^{TM} lenses had this coating effect while the PureVision^{TM} lenses simply solubilized the VE even at high concentration [9]. A similar effect can be seen regarding the VEMA and VEMA+TRIS prints, where clear phase separation was observed with the former and not the latter. Further optimization of both formulations could be done to mimic a similar study to observe how increasing VEMA concentrations may impact the EWC and if a noticeable difference in mechanisms can be observed.

The study should be repeated following the proper lens soaking procedure to minimize drug loss prior to the start of the study and observe how it impacts the release profile. A higher DXP concentration would likely contribute to a greater burst release followed by a slightly extended release duration. As seen with Figure 18, there is a negligible increase in DXP being released beyond 24hrs thus repeating the study with a higher concentration would be useful to determine whether it is possible to extend release beyond the one day mark. Additionally, a higher cumulative amount of the drug would be released, although, the cumulative percentage released may remain the same. Overall, this study helps us understand the different molecular diffusivity of the different print materials as well as understanding how the release profile may be for a MM lens with a VEMA or VEMA+TRIS embedded ring.

5.0 Conclusions

Herein, three bioinks were developed to create 3D printable contact lenses of different compositions to examine their potential use as personalized therapeutic contact lenses (TCLs). The three formulations showed unique characteristics, with noticeable differences and trends. The ATR-FTIR confirmed VEMA and TRIS were successfully incorporated into the modified lenses. The VEMA prints showed that vitamin E (VE) could directly polymerized to be a part of the lens matrix rather than absorbed through diffusion like previous studies have shown. Another noteworthy discovery was the impact of the addition of TRIS with VEMA impacts the print quality. The VEMA+TRIS prints showed significantly better print quality compared to VEMA prints with fewer defectiveness and greater homogeneity seen in the TEM images. The addition of VEMA and TRIS resulted in more hydrophobic lenses, with decreases in water content and an increase in contact angles observed. This increased content of hydrophobic moieties also resulted in an increase in stiffness as the modulus raised significantly from the base material. Furthermore, the addition of the VEMA and TRIS significantly decreased the lens transparency compared to the base material due to the increased degree of light scattering and opacity seen with the prints caused by the defects and poor miscibility, respectively. No significant differences in the release profiles were noticed, with both base and VEMA prints showing similar release profiles and similar amounts of DXP released. The amount of DXP released nearly doubled from the VEMA+TRIS lenses, indicating that the addition of TRIS reduces the degree of physical entrapment of DXP molecules within the lens matrix. The incorporation of VEMA did not show any impact on the drug release profiles which could be due to the low concentration used to examine its effect. Due to the volume required to fill the vats to a sufficient level without impacting print quality, large batches of ~80-100mL were made. Incorporating of >5% VEMA into these formulations would

require extensive synthesis and use of raw materials as it takes roughly 10g of VE to synthesize 5g of VEMA.

The multi-material (MM) prints showed a balance of the physical and mechanical properties between the base and VEMA materials. The modulus was similar to the base material and seemed to mitigate the brittle nature of the VEMA prints with a higher tensile strength and elongation profile comparatively. A similar trend can be seen with the transparency of the MM prints, whereby there is a significant improvement compared to the VEMA prints as the clear optic zone minimizes the transparency issues of the VEMA ring on the peripheral of the lens.

Future work primarily entails optimizing the lens formulations to meet commercial standards as well as changing the lens design to incorporate different base curves and utilizing a more advanced printer as the VP technology rapidly improves year-by-year. An improved printing setup with a higher resolution printer or smoother print surface could see at least the base material meet commercial standards and generally improve the transparency of the other formulations. A lower moduli could be achieved by reducing the monomer concentration or adding a diluent would make the lenses much more comfortable for users. With the present base formulation, it was seen that 3DP could produce lower moduli lenses compared to mold casting which is the most common method for commercial lens manufacturing. An alternative material to PEGDA should be explored due to its degradative properties in aqueous environments like the tear film, such as N-vinyl pyrrolidone which may also reduce the high moduli seen in all prints. The lenses do meet some commercial standards, namely, their hydrophilicity and wettability. Both VEMA and VEMA+TRIS formulations could be optimized to find a balance between improved miscibility and print quality without compromising transparency. Incorporating higher VEMA concentrations with TRIS could be worth exploring to identify an ideal ratio between the two components. The

release study should be repeated following the correct sample preparation as over an extended period. Drug release studies with the MM lens design with either a VEMA or VEMA+TRIS embedded ring would also be worth exploring to understand the impact the design may have. Once the formulations are optimized, drugs of varying charge or hydrophobicity can be incorporated and examined, followed by the incorporation of multiple drugs in a single lens. The dispersion of multiple drugs can the be localized to specific regions of the lens along with the desired material to examine the impact of MM lens design to create a tunable multi-drug loaded TCL. Finally, MTT and live/dead assays would be essential at examining the cell viability of the lenses to learn whether the materials are non-cytotoxic.

References

1. Organization, W.H. *Blindness and vision impairment*. 2023; Available from: https://www.who.int/news-room/fact-sheets/detail/blindness-and-visual-impairment#:~:text=Key%20facts,are%20refractive%20errors%20and%20cataracts.
2. Optometrists, C.A.o. *CAO Eye Health Statistics*. 2018; Available from: https://opto.ca/sites/default/files/resources/documents/eye_health_statistics_with_references_july_2019.pdf.
3. Kohane, J.B.C.T.R.H.N.G.I.I.B.C.H.D.R.L.D.S., *A Drug-Eluting Contact Lens.* Investigative Ophthalmology & Visual Science (iVOS), 2009. **50**: p. 3346-3352.
4. Xu, J., et al., *A comprehensive review on contact lens for ophthalmic drug delivery.* J Control Release, 2018. **281**: p. 97-118.
5. Lim, L. and E.W.L. Lim, *Therapeutic Contact Lenses in the Treatment of Corneal and Ocular Surface Diseases—A Review.* The Asia-Pacific Journal of Ophthalmology, 2020. **9**(6): p. 524-532.
6. Jacobs, D.S., et al., *BCLA CLEAR – Medical use of contact lenses.* Contact Lens and Anterior Eye, 2021. **44**(2): p. 289-329.
7. Rizvi, S., et al., *The role of vitamin e in human health and some diseases.* Sultan Qaboos Univ Med J, 2014. **14**(2): p. e157-65.
8. Yang, C., et al., *Recent Advances in the Application of Vitamin E TPGS for Drug Delivery.* Theranostics, 2018. **8**(2): p. 464-485.
9. Peng, C.C., J. Kim, and A. Chauhan, *Extended delivery of hydrophilic drugs from silicone-hydrogel contact lenses containing vitamin E diffusion barriers.* Biomaterials, 2010. **31**(14): p. 4032-47.
10. Shaker, L.M., A. Al-Amiery, and W.N.R.W. Isahak, *Revolutionizing contact lens manufacturing: exploring cutting-edge techniques and innovations for enhanced vision and comfort.* International Journal of Low-Carbon Technologies, 2024. **19**: p. 359-385.
11. Gu, Z., et al., *Development of 3D bioprinting: From printing methods to biomedical applications.* Asian Journal of Pharmaceutical Sciences, 2020. **15**(5): p. 529-557.
12. Bozkurt, Y. and E. Karayel, *3D printing technology; methods, biomedical applications, future opportunities and trends.* Journal of Materials Research and Technology, 2021. **14**: p. 1430-1450.
13. Tan, G., et al., *3D printing in Ophthalmology: From medical implants to personalised medicine.* International Journal of Pharmaceutics, 2022. **625**: p. 122094.
14. Xu, X., et al., *Vat photopolymerization 3D printing for advanced drug delivery and medical device applications.* J Control Release, 2021. **329**: p. 743-757.
15. Tsui, J.K.S., et al., *Applications of three-dimensional printing in ophthalmology.* Survey of Ophthalmology, 2022. **67**(4): p. 1287-1310.
16. Wang, Y., et al., *Application of Bioprinting in Ophthalmology.* Int J Bioprint, 2022. **8**(2): p. 552.
17. Alam, F., et al., *3D Printed Contact Lenses.* ACS Biomater Sci Eng, 2021. **7**(2): p. 794-803.
18. Jie Zhu, E.Z., Katia Del Rio-Tsonis, *Eye Anatomy.* John Wiley & Sons Ltd., 2012.
19. Sridhar, M.S., *Anatomy of cornea and ocular surface.* Indian Journal of Ophthalmology, 2018. **66**(2): p. 190-194.
20. Louis Tong, W.L.a.A.P., *Definition of the Ocular Surface.* Ocular Surface: Anatomy and Physiology, Disorders and Therapeutic Care, 2013: p. 3-19.
21. Craig Boote, I.A.S., Rafael Grytz, Yi Hua, Thao D. Nguyen, Michael J.A. Girard, *Scleral structure and biomechanics.* Progress in Retinal and Eye Research, 2020. **74**.
22. Derek W. DelMonte MD, T.K.M., *Anatomy and physiology of the cornea.* Journal of Cataract and Refractive Surgery, 2011. **37**(3): p. 588-598.

23. Gandhi, S. and S. Jain, *The Anatomy and Physiology of Cornea*, in *Keratoprostheses and Artificial Corneas: Fundamentals and Surgical Applications*, M.S. Cortina and J. de la Cruz, Editors. 2015, Springer Berlin Heidelberg: Berlin, Heidelberg. p. 19-25.
24. Dilly, P.N., *Structure and Function of the Tear Film*, in *Lacrimal Gland, Tear Film, and Dry Eye Syndromes: Basic Science and Clinical Relevance*, D.A. Sullivan, Editor. 1994, Springer US: Boston, MA. p. 239-247.
25. Cwiklik, L., *Tear film lipid layer: A molecular level view.* Biochim Biophys Acta, 2016. **1858**(10): p. 2421-2430.
26. Mofidfar, M., et al., *Drug delivery to the anterior segment of the eye: A review of current and future treatment strategies.* Int J Pharm, 2021. **607**: p. 120924.
27. PATRICK J. CAROLINE, F., CRAIG W. NORMAN, FCLSA *HISTORY OF CONTACT LENSES*. Contact Lens Spectrum, 2022. **37**, 52.
28. Musgrave, C.S.A. and F. Fang, *Contact Lens Materials: A Materials Science Perspective.* Materials, 2019. **12**(2): p. 261.
29. McMahon, T.T. and K. Zadnik, *Twenty-five Years of Contact Lenses: The Impact on the Cornea and Ophthalmic Practice.* Cornea, 2000. **19**(5): p. 730-740.
30. Tighe, B.J., *A Decade of Silicone Hydrogel Development: Surface Properties, Mechanical Properties, and Ocular Compatibility.* Eye & Contact Lens, 2013. **39**(1): p. 4-12.
31. Sharma, N., et al., *Contact lenses for the treatment of ocular surface diseases.* Indian J Ophthalmol, 2023. **71**(4): p. 1135-1141.
32. Hsu, K.H., S. Gause, and A. Chauhan, *Review of ophthalmic drug delivery by contact lenses.* Journal of Drug Delivery Science and Technology, 2014. **24**(2): p. 123-135.
33. Bengani, L.C., et al., *Contact lenses as a platform for ocular drug delivery.* Expert Opinion on Drug Delivery, 2013. **10**(11): p. 1483-1496.
34. Rykowska, I., et al., *Drug-Modified Contact Lenses—Properties, Release Kinetics, and Stability of Active Substances with Particular Emphasis on Cyclosporine A: A Review.* Molecules, 2024. **29**(11): p. 2609.
35. Ross, A.E., et al., *Topical sustained drug delivery to the retina with a drug-eluting contact lens.* Biomaterials, 2019. **217**: p. 119285.
36. Gote, V., et al., *Ocular Drug Delivery: Present Innovations and Future Challenges.* Journal of Pharmacology and Experimental Therapeutics, 2019. **370**(3): p. 602-624.
37. Franco, P. and I. De Marco, *Contact Lenses as Ophthalmic Drug Delivery Systems: A Review.* Polymers (Basel), 2021. **13**(7).
38. Rykowska, I., I. Nowak, and R. Nowak, *Soft Contact Lenses as Drug Delivery Systems: A Review.* Molecules, 2021. **26**(18): p. 5577.
39. Edwards, G., et al., *Molecular Mechanisms Underlying the Therapeutic Role of Vitamin E in Age-Related Macular Degeneration.* Front Neurosci, 2022. **16**: p. 890021.
40. Ambati, J. and B.J. Fowler, *Mechanisms of age-related macular degeneration.* Neuron, 2012. **75**(1): p. 26-39.
41. Sharma, P.K., et al., *Application of Vitamin E TPGS in ocular therapeutics – Attributes beyond excipient.* Journal of the Indian Chemical Society, 2022. **99**(3): p. 100387.
42. Lee, D., et al., *Ocular Drug Delivery through pHEMA-Hydrogel Contact Lenses Co-Loaded with Lipophilic Vitamins.* Scientific Reports, 2016. **6**(1): p. 34194.
43. Garg, U., et al., *The emerging role of 3D-printing in ocular drug delivery: Challenges, current status, and future prospects.* Journal of Drug Delivery Science and Technology, 2022. **76**: p. 103798.
44. Ng, W.L., et al., *Vat polymerization-based bioprinting—process, materials, applications and regulatory challenges.* Biofabrication, 2020. **12**(2): p. 022001.

45. Wang, Z., et al., *A simple and high-resolution stereolithography-based 3D bioprinting system using visible light crosslinkable bioinks.* Biofabrication, 2015. **7**(4): p. 045009.
46. Salas, A., et al., *Chemistry in light-induced 3D printing.* ChemTexts, 2023. **9**(1): p. 4.
47. Goodarzi Hosseinabadi, H., et al., *Ink material selection and optical design considerations in DLP 3D printing.* Applied Materials Today, 2023. **30**: p. 101721.
48. Gharib, G., et al., *Biomedical Applications of Microfluidic Devices: A Review.* Biosensors, 2022. **12**(11): p. 1023.
49. Martinez, P.R., et al., *Influence of Geometry on the Drug Release Profiles of Stereolithographic (SLA) 3D-Printed Tablets.* AAPS PharmSciTech, 2018. **19**(8): p. 3355-3361.
50. Shaukat, U., E. Rossegger, and S. Schlögl, *A Review of Multi-Material 3D Printing of Functional Materials via Vat Photopolymerization.* Polymers (Basel), 2022. **14**(12).
51. Robles-Martinez, P., et al., *3D Printing of a Multi-Layered Polypill Containing Six Drugs Using a Novel Stereolithographic Method.* Pharmaceutics, 2019. **11**(6).
52. Hisham, M., A.E. Salih, and H. Butt, *3D Printing of Multimaterial Contact Lenses.* ACS Biomaterials Science & Engineering, 2023. **9**(7): p. 4381-4391.
53. Tagami, T., et al., *Lyophilized ophthalmologic patches as novel corneal drug formulations using a semi-solid extrusion 3D printer.* International Journal of Pharmaceutics, 2022. **617**: p. 121448.
54. Mohamdeen, Y.M.G., et al., *Development of 3D printed drug-eluting contact lenses.* Journal of Pharmacy and Pharmacology, 2021. **74**(10): p. 1467-1476.
55. Xu, X., et al., *3D Printed Punctal Plugs for Controlled Ocular Drug Delivery.* Pharmaceutics, 2021. **13**(9): p. 1421.
56. Zhang, J., et al., *An Injectable Hydrogel Prepared Using a PEG/Vitamin E Copolymer Facilitating Aqueous-Driven Gelation.* Biomacromolecules, 2016. **17**(11): p. 3648-3658.
57. Karen K. Yeung, O., and Cindy K. Dinh, *Dissecting the Soft Contact Lens.* Review of Optometry, 2018.
58. Langis Michaud, O., *Understanding the Influence of Water Content in Soft Lenses.* Review of Optometry, 2023.
59. Read, M.L., et al., *Dynamic Contact Angle Analysis of Silicone Hydrogel Contact Lenses.* Journal of Biomaterials Applications, 2011. **26**(1): p. 85-99.
60. Tarnveer Singh Bhamra, B.J.T., *Mechanical properties of contact lenses: The contribution of measurement techniques and clinical feedback to 50 years of materials development.* Contact Lens and Anterior Eye, 2017. **40**(2): p. 70-81.
61. Anycubic. *Anycubic Photon Mono X*. Available from: https://store.anycubic.com/products/photon-mono-x-resin-printer?srsltid=AfmBOoq7I0eS8EO3hAsUhgLnp3vfMjJ3VT2vJpmv4CsZmRIIc1kyHYrV.
62. Incorporated, B.L. *DEXAMETHASONE SODIUM PHOSPHATE- dexamethasone sodium phosphate solution/ drops* National Institutes of Health (NIH) 2022; Available from: https://dailymed.nlm.nih.gov/dailymed/fda/fdaDrugXsl.cfm?setid=6bdcefbe-51e3-4ca4-afda-5aeca7b6fa73&type=display.
63. Merative, M. *Dexamethasone (Ophthalmic Route)*. Drugs and Supplements 2024; Available from: https://www.mayoclinic.org/drugs-supplements/dexamethasone-ophthalmic-route/proper-use/drg-20406621.
64. Johnson DB, L.M., Kelley B. *Dexamethasone*. StatPearls 2023; Available from: https://www.ncbi.nlm.nih.gov/books/NBK482130/.

Appendix

A1: Absolute Cumulative Amount of DXP released

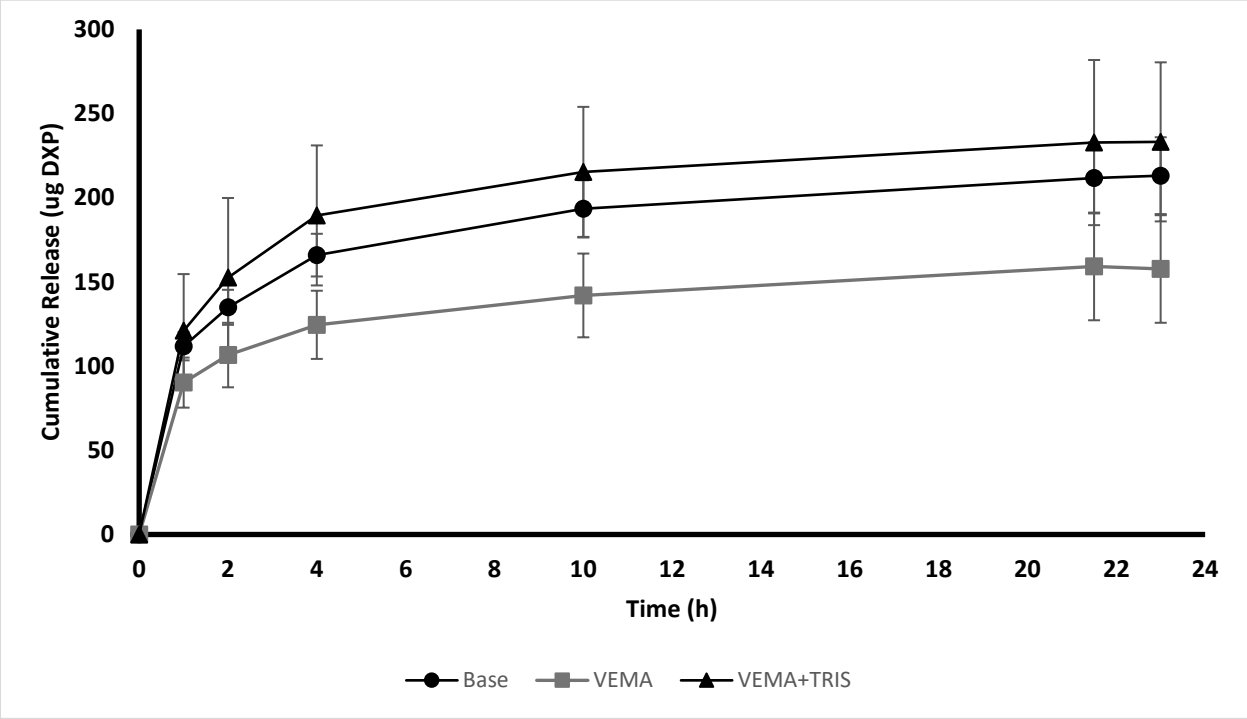

Figure 19:Absolute cumulative DXP released from single material lenses over 24hrs. Lenses were soaked in PBS at room temperature for the period of this study (n=3)

A2: Normalized Cumulative Amount of DXP released

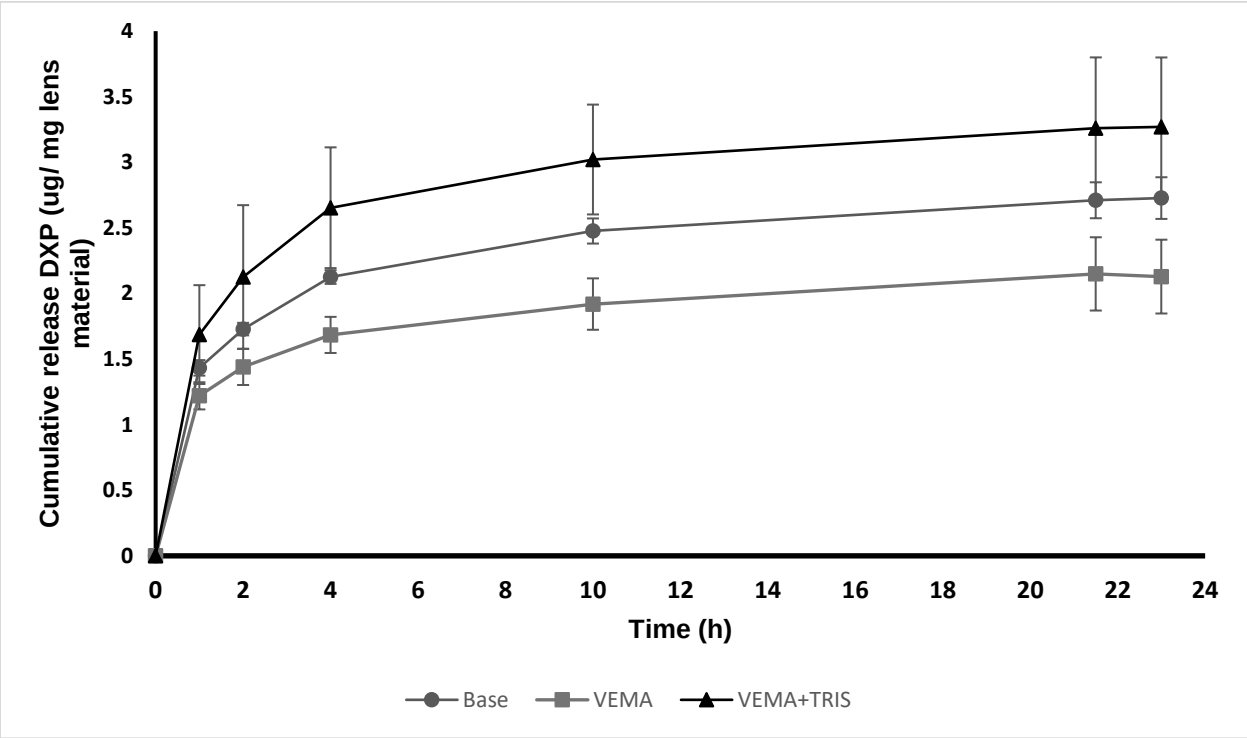

Figure 20: Normalized cumulative amount DXP per gram of lens material for single material lenses over 24hrs. Lenses were soaked in PBS at room temperature for the period of this study (n=3)